

Supporting Information for: Nuclear-weighted X-ray Maximum Entropy Method - NXMEM

Sebastian Christensen¹, Niels Bindzus¹, Mogens Christensen¹ and Bo Brummerstedt Iversen^{1*}

¹Department of Chemistry & iNANO, Aarhus University, DK-8000 Aarhus, Denmark

Table of Contents

| | |
|--|----|
| Further details for NXMEM procedure..... | 2 |
| How to calculate eNDD using <i>PRIOR</i> | 2 |
| Generation of simulated diffraction patterns | 3 |
| Additional MEM and NXMEM density plots..... | 3 |
| NXMEM and standard MEM at 300 K..... | 3 |
| Te in NXMEM and MEM | 5 |
| Improving the deconvolution | 7 |
| Alternative deconvolution factors..... | 9 |
| Finding the optimum stopping criteria..... | 10 |
| Fourier-difference maps..... | 10 |
| PbTe | 10 |
| Ba ₈ Ga ₁₆ Sn ₃₀ | 14 |
| Residual density analysis: | 17 |
| PbTe | 17 |
| Ba ₈ Ga ₁₆ Sn ₃₀ | 17 |
| Probability distribution functions from anharmonic refinements | 19 |
| Parameters for simulation..... | 20 |
| PbTe | 20 |
| Ba ₈ Ga ₁₆ Sn ₃₀ | 22 |
| Refined parameters for simplistic models..... | 23 |
| PbTe | 23 |
| Ba ₈ Ga ₁₆ Sn ₃₀ | 24 |
| Integrated charges..... | 25 |

| | |
|---|----|
| PbTe..... | 25 |
| Ba ₈ Ga ₁₆ Sn ₃₀ | 25 |
| Initial BayMEM R-values for non-uniform prior | 28 |
| BayMEM final R-values..... | 29 |
| References | 32 |

Further details for NXMEM procedure

After completing the refinement of the data, JANA2006 can automatically prepare the input file (*.BayMEM) for *BayMEM* (Tools>Files for MEM>BayMEM). The *BayMEM* file contains observed structure factors on an absolute scale which are corrected for extinction, absorption and anomalous dispersion.

The partial structure factors were calculated in *JANA2006*. To do it, go to “Refine”-menu and set “Number of cycles” = 0. Now set the occupancy of all atomic species except one to 0. When starting a refinement JANA2006 will calculate structure factors based on the current model, but will not make changes to the model. The calculated structure factors are written to the *m80* file. This file should be saved as the partial structure factors, as:

```
BGS_100K_NEXMEM_Ba.m80
BGS_100K_NEXMEM_Ga.m80
BGS_100K_NEXMEM_Sn.m80
```

The format of the *m80* file is:

```
h k l Phase Fobs Fobs norm(Fcalc) Real(Fcalc) Imag(Fcalc) ... Sigma(Fobs) Sigma(Fobs)
```

From the *m80*-files and the *BayMEM*-file $F(\mathbf{H})_{\text{obs}}^{\text{eNDD}}$ can be calculated by equations (3) and (4) from the main article. MATLAB scripts for performing NXMEM calculation based on JANA2006 output files can be made available upon request.

How to calculate eNDD using *PRIOR*

PRIOR (van Smaalen *et al.*, 2003) is built to calculate *electron density distributions* (EDD) from the analytic model of form factors:

$$f_a(\sin(\theta)/\lambda) = \sum_{i=1}^n a_i \exp\left(-b_i \frac{\sin^2(\theta)}{\lambda^2}\right)$$

where a_i and b_i are elemental specific constants which are read by *PRIOR* from the file: *factors_atomstions.fit*. The entry for each element (shown below for Pb) span 3 lines. 1st line contains the atomic number and name. The name is a case sensitive keyword used to access the entry. 2nd line contains all a_i 's and the 3rd line all b_i 's.

```
82      Pb
      31.0617    13.0637    18.4420    5.96960    13.41180    0.000000
      0.690200   2.35760    8.61800    47.2579    0.000000    0.000000
```

It is easy to modify *factors_atomsions.fit* to obtain *electron weighted nuclear density distributions* (eNDDs) since the form factor in this case is merely a constant: $f_a(\sin(\theta)/\lambda) = Z_a$. One should set $a_{i=1} = Z_a$, $a_{i \neq 1} = 0$ and $b_i = 0$ since $\exp(-0 \cdot \sin^2(\theta)/\lambda^2) = 1$. The modified entry for Pb is shown below:

| | | | | | | |
|---------|---------|---------|---------|----------|----------|--|
| 82 | ePb | | | | | |
| 82.0000 | 0.00000 | 0.00000 | 0.00000 | 0.000000 | 0.000000 | |
| 0.00000 | 0.00000 | 0.00000 | 0.00000 | 0.000000 | 0.000000 | |

The keyword is changed to ePb to make the entry unique. Similarly, one can include neutron scattering lengths to obtain neutron-scattering-length density distribution.

Generation of simulated diffraction patterns

The simulated data were scaled to have same intensity as our actual SPring8 data on PbTe and a flat background was added. Normal distributed noise was added to the simulated data. In the SPring8 data the standard uncertainty, $\sigma(2\theta)$, on the intensity is estimated as $\sigma(2\theta) = \sqrt{I(2\theta)}$. However we chose the width of the normal distribution to be $\sigma(2\theta)/3$ since this gave a signal-to-noise ratio comparable to the actual data in the high-angle region. The reason for the reduced normal distribution width may be attributed to the fact that the experimental data were recorded on a logarithmic scale on an image plate detector.

Additional MEM and NXMEM density plots

NXMEM and standard MEM at 300 K

The spatial distributions of the 300 K eNDDs calculated by NXMEM are shown in Figure 2 (top) for the Pb site. As a reference, we also show the true eNDD, Figure 2 (bottom). The NXMEM eNDDs are in general in good agreement with the reference. Due to thermal motion, the Pb displacement is only resolved for $x = 0.04$. However for $x = 0.03$ the asperic density indicates the direction of displacement.

The EDD determined by standard MEM are shown in Figure 3 (top). For $x = 0.04$ the EDD of Pb is distorted but the off-centre position is not resolved. Therefore NXMEM also appears superior to standard MEM for disordered structures at 300 K.

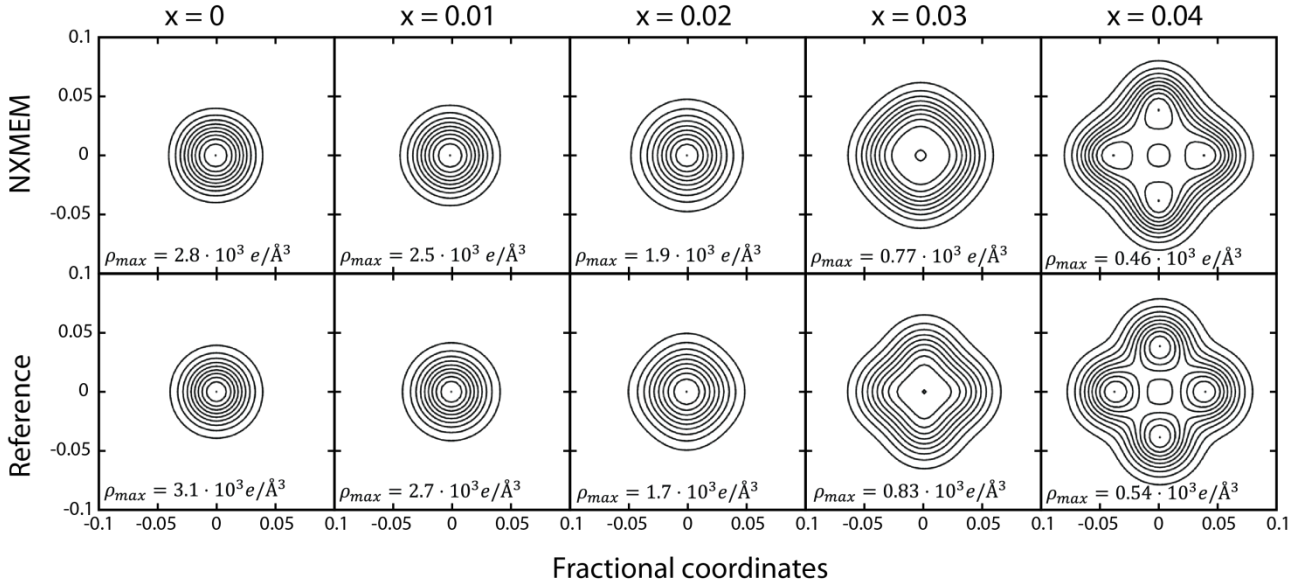


Figure 1 (top) NXMEM eNDDs of Pb in the (001)-plane through the 4b position. (bottom) Reference eNDD calculated from the true structure. Contour lines are drawn in steps of $\rho_{max}/10$, where ρ_{max} is the maximum density of the map.

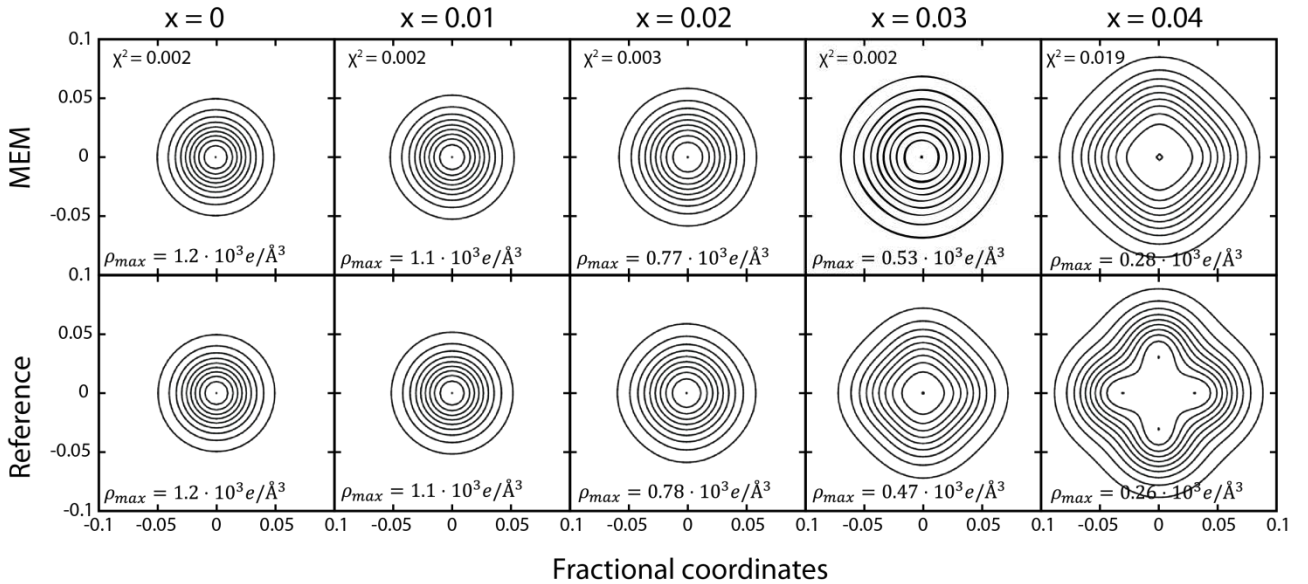


Figure 2 (top) MEM EDDs of Pb in the (001)-plane through the centre of 4b position. For $x=0.04$, it was necessary to use a non-uniform prior based on the refined isotropic model to reach a satisfying χ^2 -value. (bottom) Reference EDDs calculated from the true structure. Contour lines are drawn in steps of $\rho_{max}/10$, where ρ_{max} is the maximum density of the map.

Table 1 Results from EDMA for MEM and NXMEM calculations on PbTe (Palatinus *et al.*, 2012)

| Uniform prior | | | | | | | | |
|--------------------|------------------|--------------|------------------|---------------------|------------------|---------------------|------------------|---------------------|
| | 100 K | | | | 300 K | | | |
| x_{model} | x_{max} | $\Delta x/x$ | x_{coc} | $\Delta x/x$ (%) | x_{max} | $\Delta x/x$ (%) | x_{coc} | $\Delta x/x$ (%) |
| NXMEM | 0.03 | 0.0277 | -7.65% | 0.0298 | -0.57% | 0 | - | 0 - |
| | 0.04 | 0.0504 | 25.98% | 0.0415 | 3.78% | 0.0380 | -5.06% | 0.0416 4.08% |
| MEM | 0.04 | - | - | - | - | 0 | - | 0 - |

| Non-uniform prior | | | | | | | | |
|--------------------|------------------|--------------|------------------|---------------------|------------------|---------------------|------------------|---------------------|
| | 100 K | | | | 300 K | | | |
| x_{model} | x_{max} | $\Delta x/x$ | x_{coc} | $\Delta x/x$ (%) | x_{max} | $\Delta x/x$ (%) | x_{coc} | $\Delta x/x$ (%) |
| NXMEM | 0.03 | 0.0214 | -28.67% | 0.0296 | -1.17% | 0 | - | 0 - |
| | 0.04 | 0.0446 | 11.42% | 0.0386 | -3.53% | 0.0384 | -4.09% | 0.0416 4.12% |
| MEM | 0.04 | 0.0115 | -71.32% | 0.0588 | 47.07% | 0 | - | 0 - |

Te in NXMEM and MEM

In all test structures Te was kept at the high symmetry position $4a$, thus the NXMEM eNDD of Te was expected to be centred at $4a$ and spherical in all cases. However, for $x \geq 0.03$ the eNDD of Te becomes slightly distorted in the $\langle 100 \rangle$ -directions, Figure 4. Nonetheless, in all cases the distortions are much smaller than for Pb. The erroneous Te distortions could be diminished and even removed by using a non-uniform prior based on the isotropic refined model.

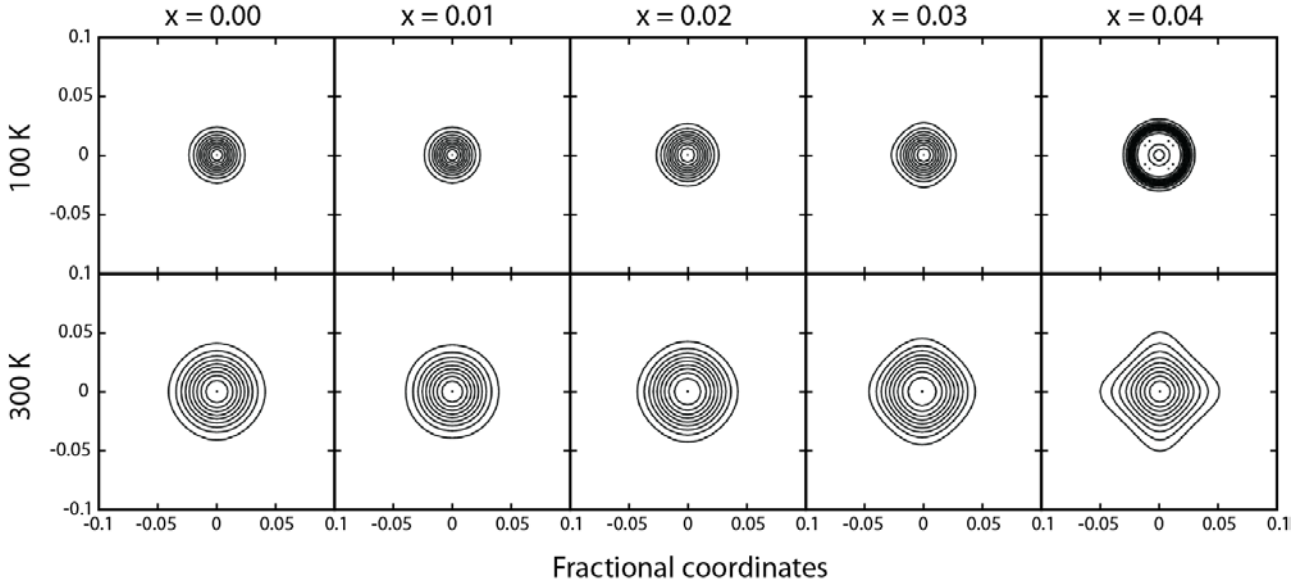


Figure 3 NXMEM eNDDs of Te in the (001)-plane through the $4a$ position at 100 K (top) and 300 K (bottom).

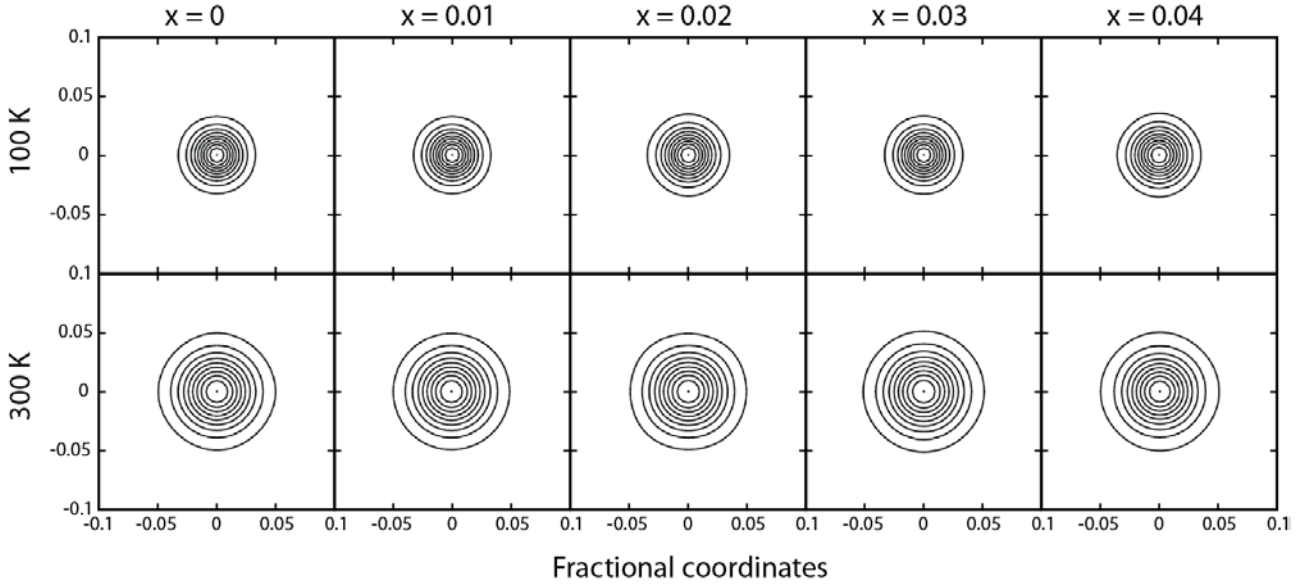


Figure 4 Standard MEM EDDs of Te in the (001)-plane through the 4a position at 100 K (top) and 300 K (bottom).

NXMEM and standard MEM at 100 K with non-uniform prior

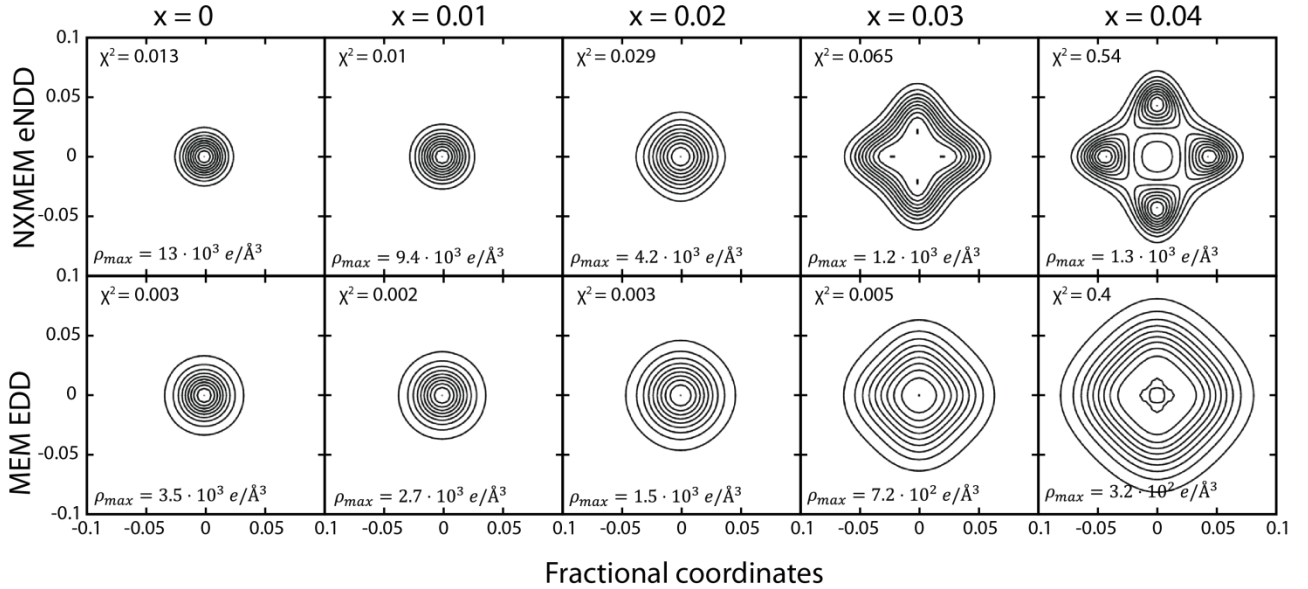


Figure 5 (top) NXMEM eNDDs and (bottom) MEM EDD of Pb in the (001)-plane through the 4b position. In both cases a non-uniform prior density calculated from the simplistic model was used. Contour lines are drawn in steps of $\rho_{max}/10$, where ρ_{max} is the maximum density of the map.

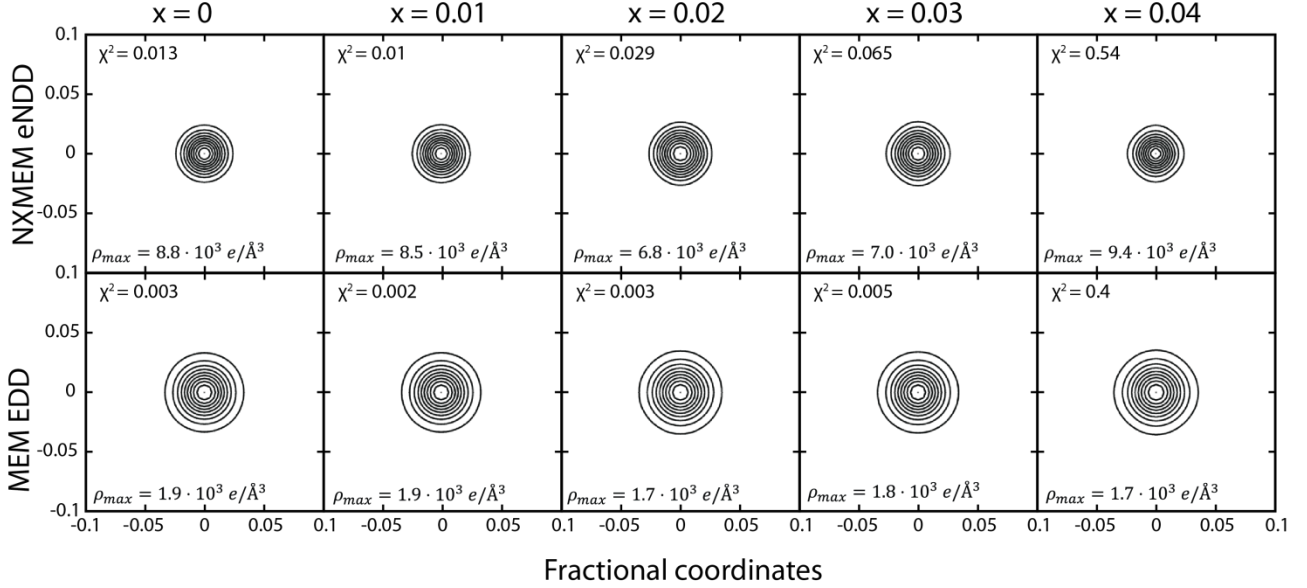


Figure 6 (top) NXMEM eNDDs and (bottom) MEM EDDs of Te in the (001)-plane through the 4b position. In both cases a non-uniform prior density calculated from the simplistic model was used. Contour lines are drawn in steps of $\rho_{max}/10$, where ρ_{max} is the maximum density of the map.

Improving the deconvolution

The accuracy of both the extracted F_{obs} and the deconvolution factors, df , depend on the model. In the main paper, we show that a simple isotropic model without displacement (“iso-model”) is sufficient to perform NXMEM calculations which yield quantitative information, Figure 6 (iso,iso).

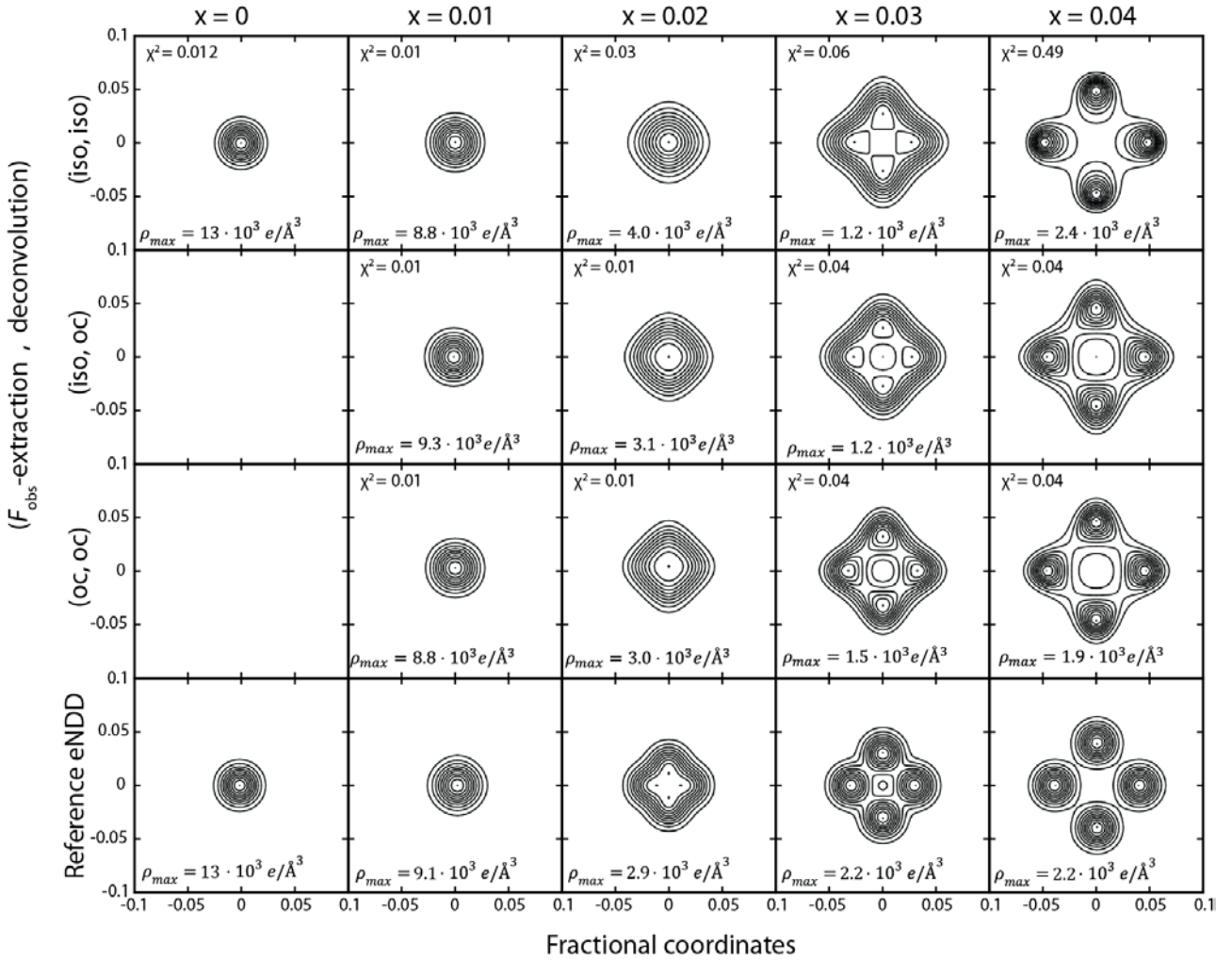


Figure 7 NXMEM eNDD of Pb (1st row) F_{obs} -extraction and deconvolution factor based on iso-model. (2nd row) F_{obs} -extraction based on iso-model and deconvolution factor based on oc-model. (3rd row) F_{obs} -extraction and deconvolution factors based on oc-model. (4th row) The reference eNDD.

The simulated data were refined with a model that included displacement of Pb (“oc-model”). The oc-model was used to calculate accurate deconvolution factors, df_{oc} . These were combined with structure factors extracted with the “iso-model”, $F_{obs,iso}$ to perform NXMEM calculations, Figure 6 (iso, oc). The distortion of $x = 0.02$ becomes slightly more pronounced and the off-center maxima become more clearly defined for $x = 0.03$. To improve the deconvolution further we also used the oc-model to extract structure factors, $F_{obs,oc}$. The NXMEM calculations based on $F_{obs,oc}$ and df_{oc} , Figure 6 (oc, oc), are further improved. For both (iso, oc)- and (oc, oc)-calculations with $x = 0.04$ it was necessary to use non-uniform prior (isotropic model) to properly converge the density. Therefore, it might be fortuitous that a non-uniform prior was not necessary in the $= 0.04$, (iso, iso)-calculation.

The results of Figure 6 clearly demonstrate that by using a more accurate model in each step of NXMEM, it is possible to systematically improve the eNDD.

Alternative deconvolution factors

In addition to weighting based on the structure factor, equation (2) which was used in the main article, we tested two additional weighting methods. These were based on the norm of structure factor, equation (2) and on the Morningstar-Warren approximation known from total scattering, equation (2)

$$df(\mathbf{H}) = \sum_j w_j(\mathbf{H}) \frac{Z_j}{f_j(H)} \quad (1)$$

| | | |
|--------------------|----|---|
| F weight | a) | $w_j(\mathbf{H}) = \frac{F_{model,j}^{EDD}(\mathbf{H})}{F_{model}^{EDD}(\mathbf{H})}$ |
| F-norm weight | b) | $w_j(\mathbf{H}) = \frac{ F_{model,j}^{EDD}(\mathbf{H}) }{ F_{model}^{EDD}(\mathbf{H}) }$ |
| Morningstar-Warren | c) | $w_j(\mathbf{H}) = \frac{n_j}{\sum_j n_j}$ |

n_j is the number of atoms of element j .

(2)

The alternative weighting schemes were tested on the 100 K data with $x = 0.00$ and $x = 0.03$. NXMEM calculations were performed with uniform prior and settings identical to the calculations presented in the main article. Cuts through the density of the Pb atoms are presented in Figure 7. For $x = 0.00$ both “F-norm weight” and “Morningstar-Warren” show clear deficiencies by splitting the peak in disagreement with the true model structure. For $x = 0.03$ the results are comparable to the results obtained by “F weight”.

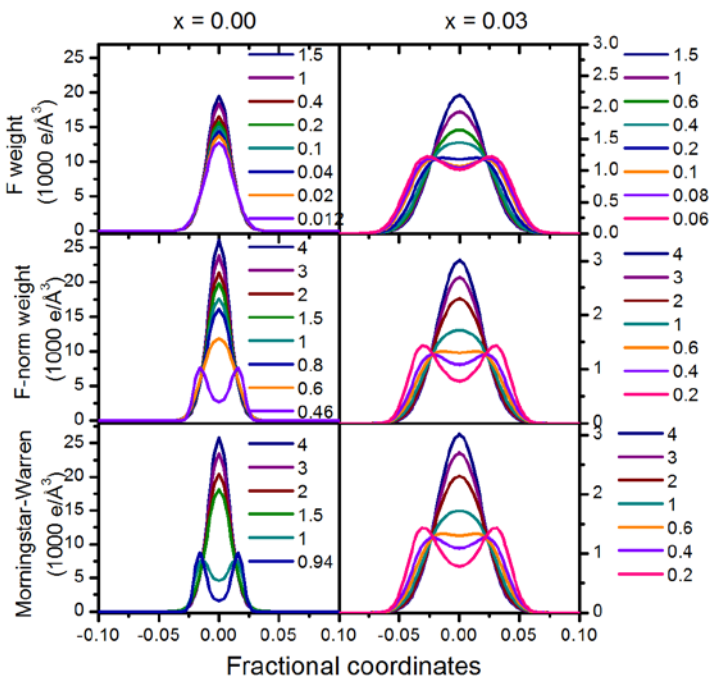


Figure 8 Cross section for multiple stopping criteria χ^2 through the Pb density using 3 different weighting schemes for the deconvolution factor. The weighting schemes are defined in equation 2.

Finding the optimum stopping criteria

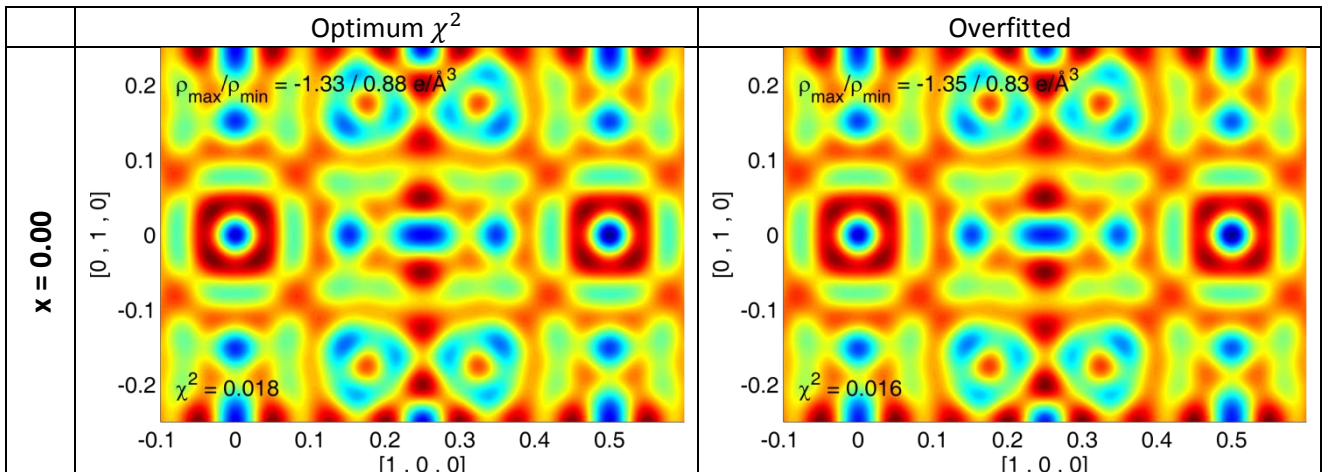
MEM and NXMEM densities on $\text{Ba}_8\text{Ga}_{16}\text{Sn}_{30}$ clearly expressed signs of overfitting at $\chi^2 \approx 1$. We tested both Fourier-difference (FD) maps and RDA for determining the optimum stopping criteria χ^2 (Hofmann *et al.*, 2007, Bindzus & Iversen, 2012). For $\text{Ba}_8\text{Ga}_{16}\text{Sn}_{30}$, it was clear that RDA could not identify overfitting since it in all cases favoured the lowest χ^2 . The stopping criteria was finally chosen by inspecting Fourier-difference maps similar to the procedure of Hofmann *et al.* (2007).

Fourier-difference maps

PbTe

For PbTe we analysed the (001)-plane containing the $4a$ (0,0,0) and $4b$ (0.5,0,0) positions. For large χ^2 the highest peaks in the FD-map are close to the $4a$ and $4b$ positions and is thus interpreted as unfitted atomic density. For lower χ^2 , peaks of comparable height emerge away from the atomic positions. These are interpreted as noise introduced by systematic errors in the data. Consequently, we conclude that the optimal MEM solution has been reached at this χ^2 . In Tables 2 and 3 are shown exerts from FD-maps for NXMEM calculations on PbTe. The left column contain FD-maps for the optimum χ^2 -value, while the right column contain FD-maps which are slightly overfitted i.e. too low χ^2 . The FD-map of the optimum χ^2 -value is characterised by having its maximum values close to the atomic position, while the highest value in the “noise region” i.e. away from atomic sites are slightly smaller. In some cases did the lowest obtainable χ^2 -value not show evidence of overfitting e.g. $x = 0.02$ & 0.03 in Table 2. Consequently this value was selected as the optimum.

Table 2 Fourier difference maps of NXMEM calculations at 100 K. The depicted plane is (001) with origin at Te (0, 0, 0).



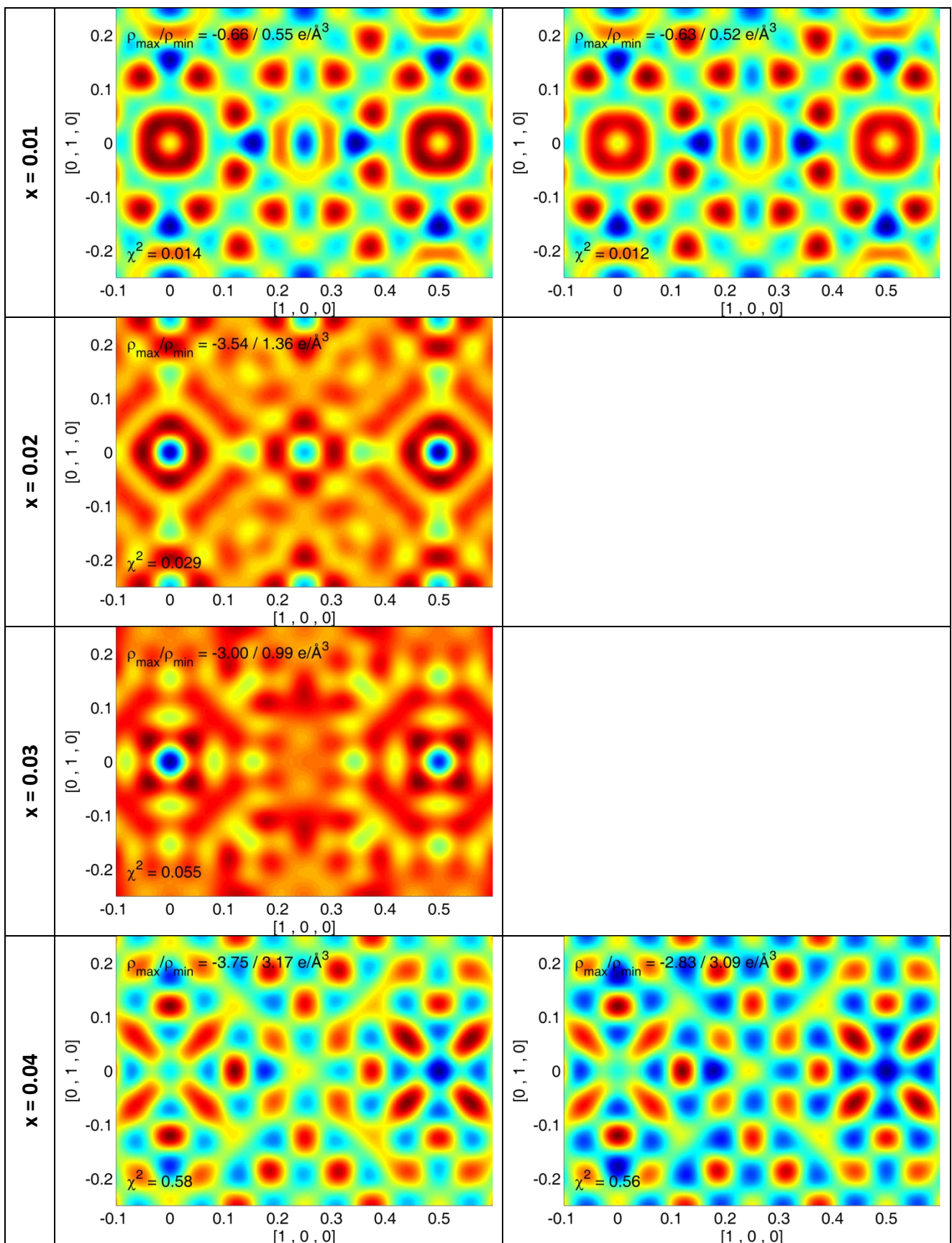
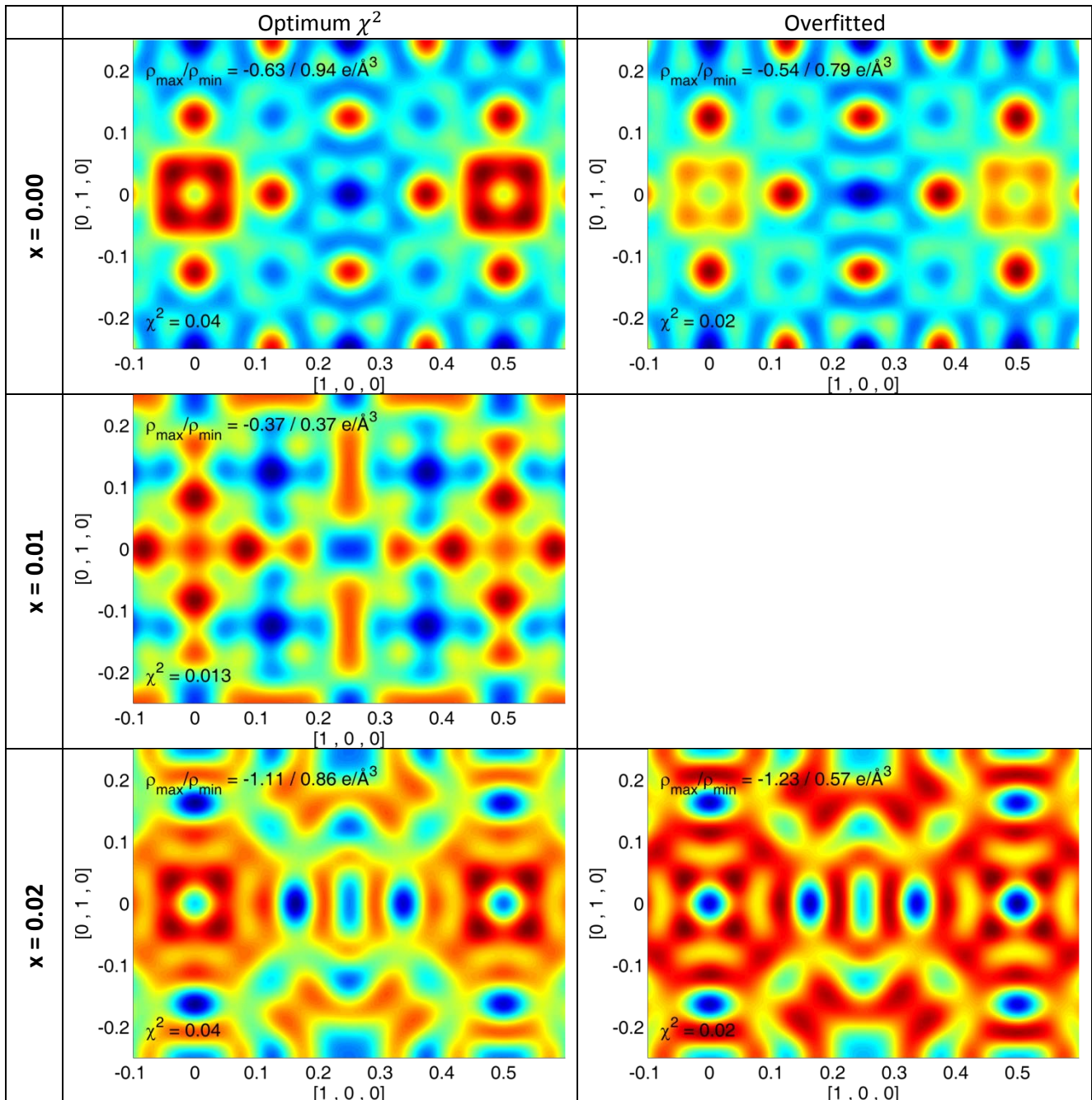
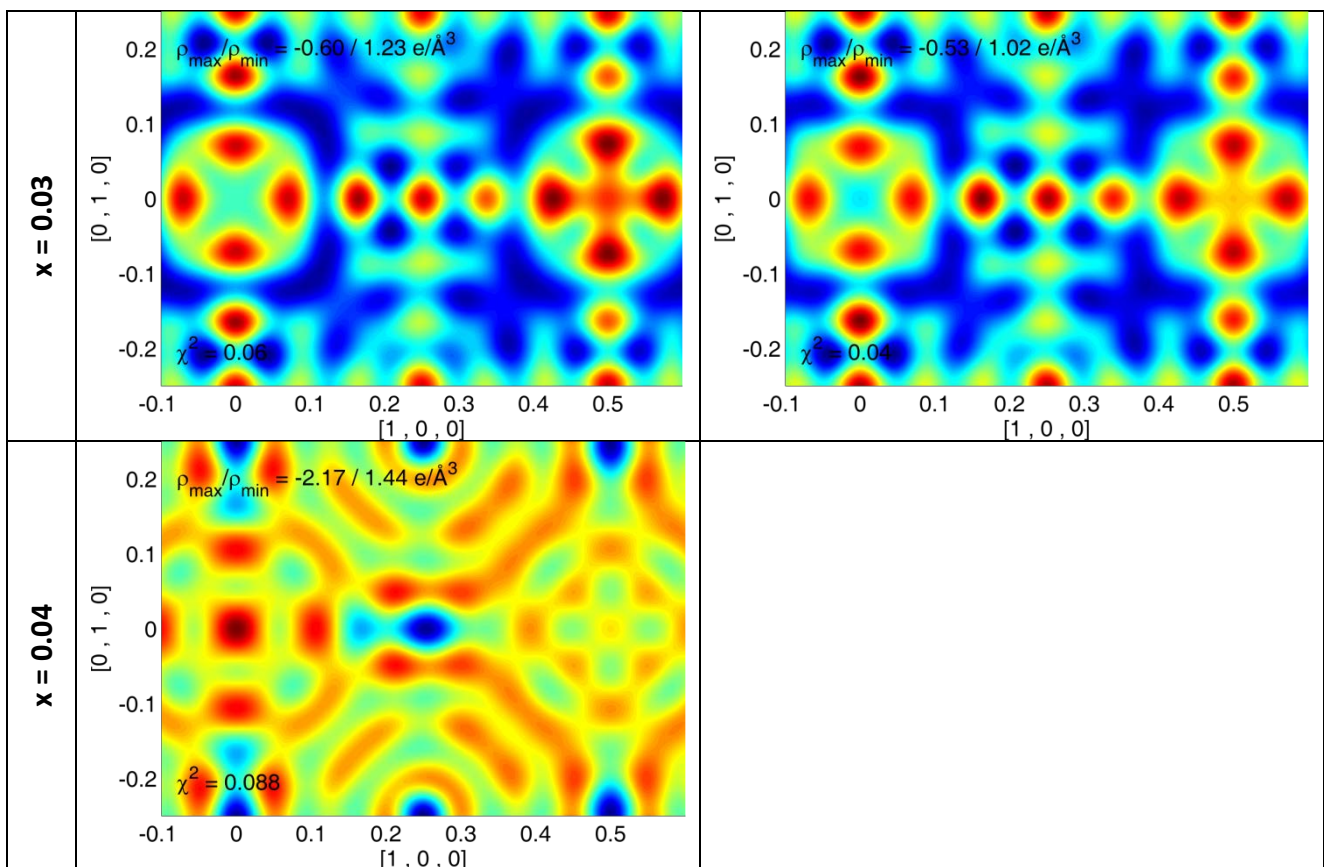


Table 3 Fourier difference maps of NXMEM calculations at 300 K. The depicted plane is (001) with origin at Te (0, 0, 0).

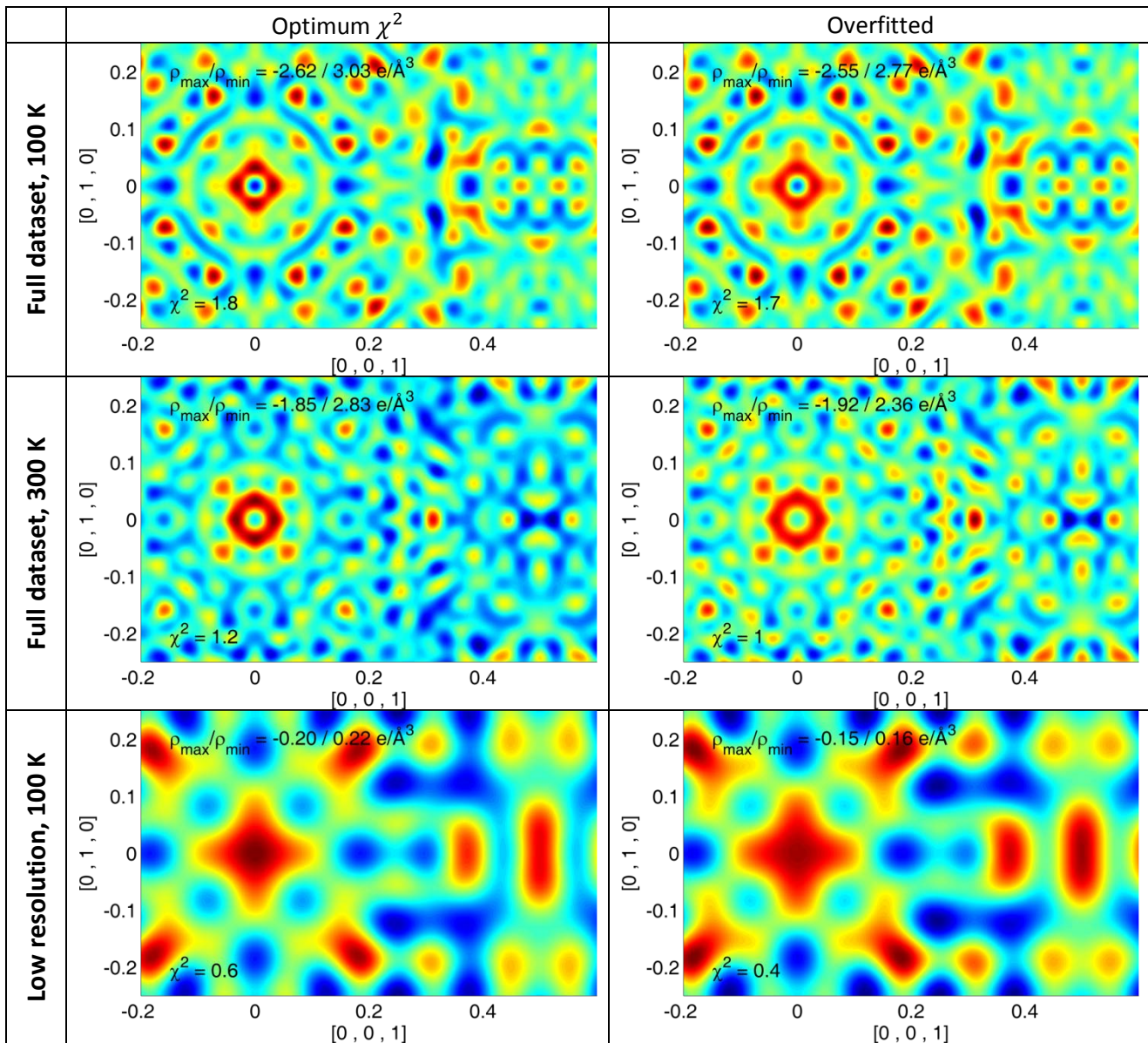




Ba₈Ga₁₆Sn₃₀

For Ba₈Ga₁₆Sn₃₀ we analyse the (100)-plane containing the 6*b* position (0.25,0.5,0) at the origin. This is the only atomic site in FD-map so all regions away from the origin are therefore to be considered noise.

Table 4 Fourier difference maps of NXMEM calculations on simulated data. The depicted plane is (100) with origin at (0.25, 0.5, 0) around which the Ba2 atom is distributed



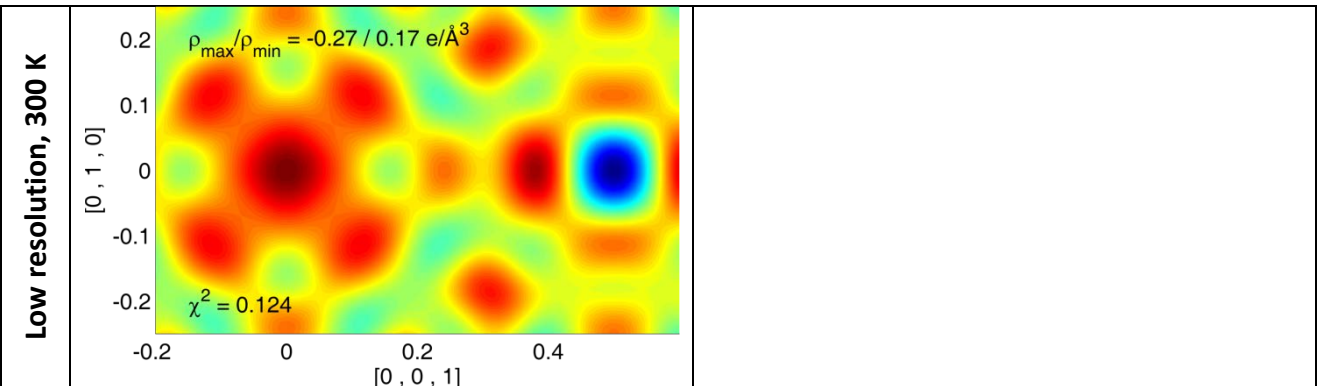
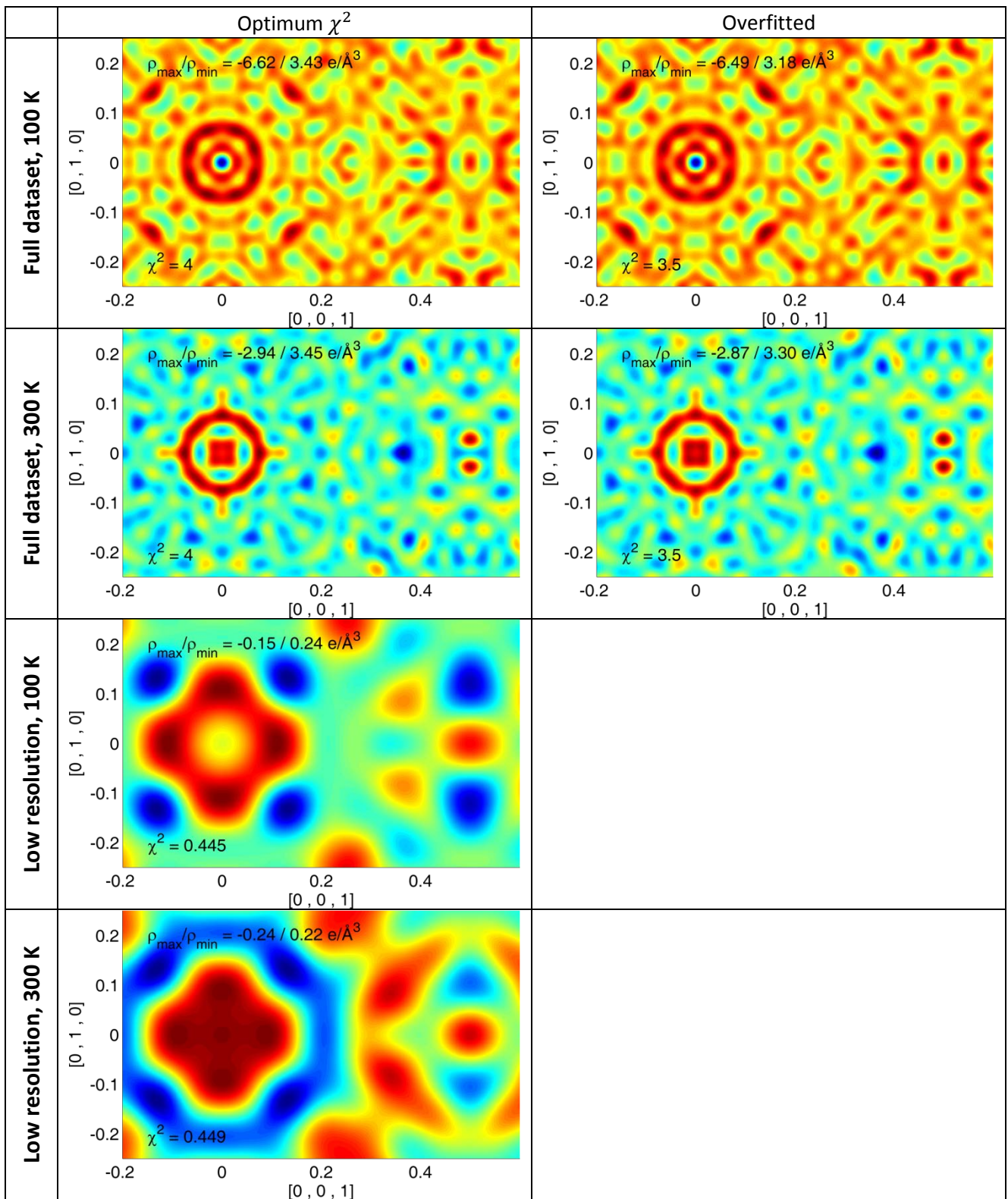


Table 5 Fourier difference maps of NXMEM calculations on experimental data. The depicted plane is (100) with origin at (0.25, 0.5, 0) around which the Ba2 atom is distributed



Residual density analysis:

Residual density analysis (RDA) has been used to determine the optimal stopping criteria, χ^2 for MEM calculations.(Bindzus & Iversen, 2012) The optimal MEM solution should have a parabolic fractal dimension plot which corresponds to a Gaussian distribution of residual density.

PbTe

The fractal dimensions for selected NXMEM calculations based on 100 K PbTe data using uniform prior are shown in Figure 8. Increasing Pb displacements clearly affects the fractal dimension by introducing non-parabolic features in the left side of the plot. Non-parabolic features are a sign of systematic errors in the data. This is somewhat expected due to the approximate nature of the NXMEM deconvolution factor. Despite not being parabolic the lowest value of χ^2 results in the most symmetric and narrow fractal dimension plot in all cases. This is in contrast to the Fourier-difference method, which in several cases indicates that the lowest χ^2 -overfits the data.

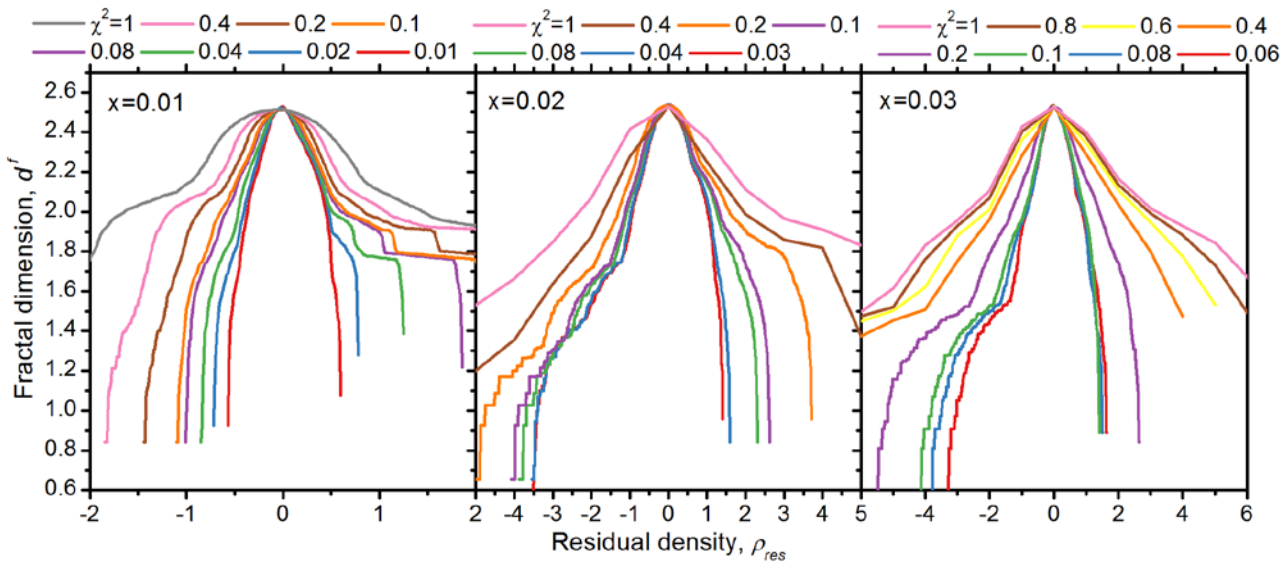


Figure 9 Fractal dimension plots for NXMEM solutions for $x = 0.01, 0.02, \& 0.03$ at 100 K using various stopping criteria, χ^2 based. The optimal MEM solution has a parabolic fractal dimension plot; however it is clearly not achieved for increased displacements, x . Non-parabolic fractal dimension plots indicate systematic errors in the data.

Ba₈Ga₁₆Sn₃₀

As an example, Figure 9 shows selected NXMEM calculations based on experimental Ba₈Ga₁₆Sn₃₀ data. For the lowest values of χ^2 does the fractal dimension approach a parabolic shape. However; the eNDD showed strong signs of overfitting. Inspection of FD-maps also showed that mainly noise was fitted for $\chi^2 < 4$. We therefore concluded that RDA was not a suitable method for determining the optimum stopping criteria in the present case.

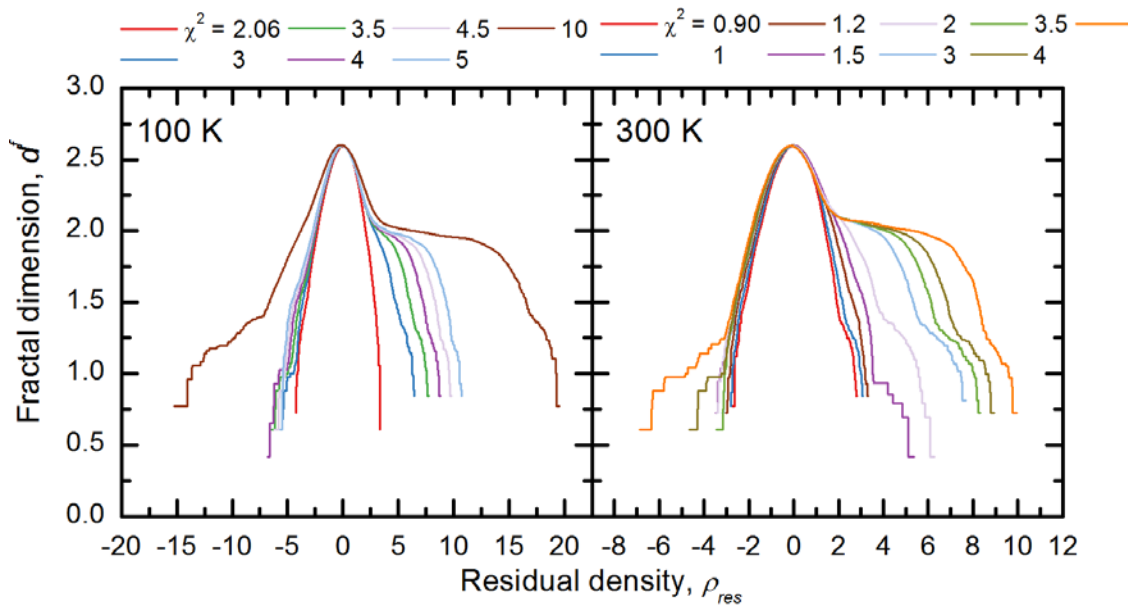


Figure 10 Fractal dimension plots for NXMEM calculations applied to the full experimental $\text{Ba}_8\text{Ga}_{16}\text{Sn}_{30}$ dataset using various stopping criteria, χ^2 .

Probability distribution functions from anharmonic refinements

The data discussed in the main paper was also refined against a model which included 4th order Gram-Charlier coefficients for the thermal motion of Pb (Kuhs, 2003). The probability density function (p.d.f.) for Pb is calculated for all datasets in Figure 10. The Pb density is distorted corresponding to the Pb displacement for $x \geq 0.02$ at 100 K and for $x \geq 0.03$ at 300 K. For $x = 0.03$ & 0.04 off-centre maxima emerge at $x_{p.d.f.} = 0.0184$ & 0.0338. For $x = 0.04$, 300 K the maximum is at $x_{p.d.f.} = 0.0069$. Only for $x = 0.04$ at 100 K the maxima position extracted from the p.d.f. are closer to the true Pb displacement compared to NXMEM.

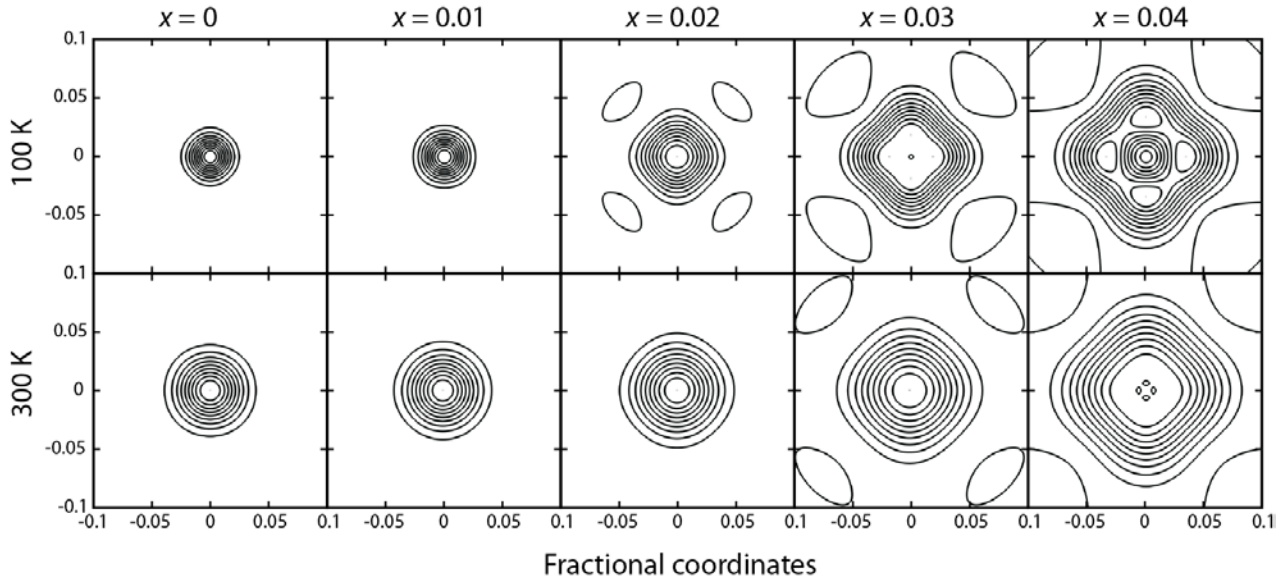


Figure 11 Probability density functions (p.d.f) in the (100) plane through the Pb atom in $(\frac{1}{2}, \frac{1}{2}, \frac{1}{2})$ obtained from anharmonic thermal parameters against the simulated data.

Parameters for simulation

PbTe

| x = | 100 K | | | | |
|--|----------|-----------|-----------|-----------|-----------|
| | 0 | 0.01 | 0.02 | 0.03 | 0.04 |
| Scale | 3.36E+05 | 3.36E+05 | 3.36E+05 | 3.36E+05 | 3.36E+05 |
| Constant | | | | | |
| background0 | 3600 | 3600 | 3600 | 3600 | 3600 |
| asym1 = asym2 | 0.001 | 0.001 | 0.001 | 0.001 | 0.001 |
| asym3 = asym4 | 0.001983 | 0.001983 | 0.001983 | 0.001983 | 0.001983 |
| a (Å) | 6.435489 | 6.435489 | 6.435489 | 6.435489 | 6.435489 |
| W - Gauss | 2.603433 | 2.603433 | 2.603433 | 2.603433 | 2.603433 |
| LX - Lorentz | 0.481563 | 0.481563 | 0.481563 | 0.481563 | 0.481563 |
| LY - Lorentz | 8.79347 | 8.79347 | 8.79347 | 8.79347 | 8.79347 |
| Dzeta | 0.598705 | 0.598705 | 0.598705 | 0.598705 | 0.598705 |
| - | - | - | - | - | - |
| St400 | 0.039529 | -0.039529 | -0.039529 | -0.039529 | -0.039529 |
| St103 | 0.197784 | 0.197784 | 0.197784 | 0.197784 | 0.197784 |
| x(Te) | 0 | 0 | 0 | 0 | 0 |
| y(Te) | 0 | 0 | 0 | 0 | 0 |
| z(Te) | 0 | 0 | 0 | 0 | 0 |
| U ₁₁ (Te) | 0.0053 | 0.0053 | 0.0053 | 0.0053 | 0.0053 |
| x(Pb) | 0.5 | 0.51 | 0.52 | 0.53 | 0.54 |
| y(Pb) | 0.5 | 0.5 | 0.5 | 0.5 | 0.5 |
| z(Pb) | 0.5 | 0.5 | 0.5 | 0.5 | 0.5 |
| U ₁₁ (Pb) (Å ²) | 0.0053 | 0.0053 | 0.0053 | 0.0053 | 0.0053 |

| X = | 300 K | | | | |
|---|-----------|-----------|-----------|-----------|-----------|
| | 0 | 0.01 | 0.02 | 0.03 | 0.04 |
| Scale | 3.36E+05 | 3.36E+05 | 3.36E+05 | 3.36E+05 | 3.36E+05 |
| Constant | | | | | |
| background0 | 3600 | 3600 | 3600 | 3600 | 3600 |
| <i>asym1 = asym2</i> | 0.001 | 0.001 | 0.001 | 0.001 | 0.001 |
| <i>asym3 = asym4</i> | 0.001983 | 0.001983 | 0.001983 | 0.001983 | 0.001983 |
| <i>a</i> (Å) | 6.435489 | 6.435489 | 6.435489 | 6.435489 | 6.435489 |
| <i>W - Gauss</i> | 2.603433 | 2.603433 | 2.603433 | 2.603433 | 2.603433 |
| <i>LX - Lorentz</i> | 0.481563 | 0.481563 | 0.481563 | 0.481563 | 0.481563 |
| <i>LY - Lorentz</i> | 8.79347 | 8.79347 | 8.79347 | 8.79347 | 8.79347 |
| <i>Dzeta</i> | 0.598705 | 0.598705 | 0.598705 | 0.598705 | 0.598705 |
| <i>St400</i> | -0.039529 | -0.039529 | -0.039529 | -0.039529 | -0.039529 |
| <i>St103</i> | 0.197784 | 0.197784 | 0.197784 | 0.197784 | 0.197784 |
| <i>x(Te)</i> | 0 | 0 | 0 | 0 | 0 |
| <i>y(Te)</i> | 0 | 0 | 0 | 0 | 0 |
| <i>z(Te)</i> | 0 | 0 | 0 | 0 | 0 |
| <i>U₁₁(Te)</i> | 0.014 | 0.014 | 0.014 | 0.014 | 0.014 |
| <i>x(Pb)</i> | 0.5 | 0.51 | 0.52 | 0.53 | 0.54 |
| <i>y(Pb)</i> | 0.5 | 0.5 | 0.5 | 0.5 | 0.5 |
| <i>z(Pb)</i> | 0.5 | 0.5 | 0.5 | 0.5 | 0.5 |
| <i>U₁₁(Pb) (Å²)</i> | 0.014 | 0.014 | 0.014 | 0.014 | 0.014 |

Ba₈Ga₁₆Sn₃₀

p-1BGS "24k model"

| | | | |
|------------------|----------------------------|----------------------------|------------------|
| Temperature (K) | | 100 | 300 |
| N_{par} | | 19 | 19 |
| N_{obs} | | 1452 | 1464 |
| a (Å) | | 11.6939 | 11.7163 |
| Extinction | | 0 | 0 |
| Ba(1) 2a | | U_{11} (Å ²) | 0.0110 0.0219 |
| Ba(2) 6d | X | 0.2543 | 0.2538 |
| | Y | 0.5409 | 0.5378 |
| | U_{11} (Å ²) | 0.0335 | 0.0499 |
| Sn/Ga(1) 6c | $a[\text{Sn}1]$ | 0.040 | 0.042 |
| | U_{11} (Å ²) | 0.0126 | 0.0213 |
| | U_{22} (Å ²) | 0.0120 | 0.0197 |
| Sn/Ga(2) 16i | $a[\text{Sn}2]$ | 0.218 | 0.216 |
| | x | 0.18410 | 0.18419 |
| | U_{11} (Å ²) | 0.0105 | 0.0187 |
| Sn/Ga(3) 24k | U_{12} (Å ²) | -0.00013 | -0.00076 |
| | Y | 0.31241 | 0.31230 |
| | Z | 0.11837 | 0.11836 |
| | U_{11} (Å ²) | 0.0126 | 0.0215 |
| | U_{22} (Å ²) | 0.0099 | 0.0178 |
| | U_{33} (Å ²) | 0.0095 | 0.0169 |
| | U_{23} (Å ²) | -0.0009 | -0.0015 |

Parameters taken from (Christensen *et al.*, 2013)

Refined parameters for simplistic models

PbTe

100 K

| | $X =$ | 0 | 0.01 | 0.02 | 0.03 | 0.04 |
|--|-------|-------------|-------------|-------------|-------------|-------------|
| $R_{\text{obs}}/wR_{\text{obs}}$ ($I_{\text{obs}} > 3\sigma_{\text{obs}}$) (%) | | 0.21/0.27 | 0.18/0.25 | 0.56/0.78 | 1.91/1.78 | 6.63/6.19 |
| $R_{\text{all}}/wR_{\text{all}}$ (%) | | 0.21/0.27 | 0.21/0.26 | 0.66/0.80 | 2.38/1.85 | 7.00/6.22 |
| R_p/wR_p (%) | | 0.36/0.47 | 0.36/0.47 | 0.37/0.49 | 0.48/0.62 | 0.78/1.15 |
| χ^2 | | 0.34 | 0.33 | 0.34 | 0.43 | 0.78 |
| Constant background | | 3599.6(3) | 3599.4(3) | 3598.3(3) | 3598.6(4) | 3605.1(7) |
| asym3=asym4 | | 0.001903(6) | 0.001902(6) | 0.001899(6) | 0.001902(8) | 0.00191(2) |
| a (Å) | | 6.435482(3) | 6.435478(3) | 6.435477(3) | 6.435480(4) | 6.435487(8) |
| W - Gauss | | 2.615(3) | 2.611(3) | 2.602(3) | 2.608(3) | 2.606(6) |
| LX - Lorentz | | 0.479(3) | 0.482(3) | 0.491(3) | 0.505(4) | 0.522(8) |
| LY - Lorentz | | 8.79(3) | 8.76(3) | 8.72(3) | 8.52(5) | 8.31(9) |
| Dzeta | | 0.5998(8) | 0.5982(8) | 0.5986(8) | 0.596(1) | 0.591(2) |
| St400 | | -0.0396(4) | -0.0394(4) | -0.0404(4) | -0.0419(6) | -0.046(1) |
| St220 | | 0.1978(3) | 0.1982(3) | 0.1988(4) | 0.2005(5) | 0.2026(9) |
| $U_{\text{iso}}(\text{Te})$ | | 0.00529(1) | 0.00532(1) | 0.00546(2) | 0.00596(2) | 0.00618(4) |
| $U_{\text{iso}}(\text{Pb})$ | | 0.005308(8) | 0.006683(9) | 0.01103(1) | 0.01859(2) | 0.03045(6) |
| Scale | | 0.21484(2) | 0.21517(2) | 0.21646(2) | 0.21872(3) | 0.22227(6) |

300 K

| | $X =$ | 0 | 0.01 | 0.02 | 0.03 | 0.04 |
|--|-------|-------------|-------------|-------------|-------------|-------------|
| $R_{\text{obs}}/wR_{\text{obs}}$ ($I_{\text{obs}} > 3\sigma_{\text{obs}}$) (%) | | 0.21/0.23 | 0.16/0.20 | 0.56/0.61 | 1.91/1.78 | 6.10/6.19 |
| $R_{\text{all}}/wR_{\text{all}}$ (%) | | 0.21/0.23 | 0.21/0.22 | 0.66/0.63 | 2.38/1.85 | 7.00/4.64 |
| R_p/wR_p (%) | | 0.36/0.47 | 0.36/0.47 | 0.37/0.49 | 0.48/0.62 | 0.78/1.15 |
| χ^2 | | 0.34 | 0.33 | 0.34 | 0.43 | 0.78 |
| Constant background | | 3599.8(3) | 3599.9(3) | 3599.4(3) | 3598.5(3) | 3600.2(4) |
| asym3=asym4 | | 0.001896(6) | 0.001891(6) | 0.001896(6) | 0.001894(7) | 0.00190(1) |
| A | | 6.435472(3) | 6.435471(3) | 6.435471(3) | 6.435476(4) | 6.435479(6) |
| Gauss - GW | | 2.613(3) | 2.613(3) | 2.608(3) | 2.608(3) | 2.611(4) |
| Lorentz – LX | | 0.484(3) | 0.481(3) | 0.487(4) | 0.497(4) | 0.507(6) |
| Lorentz – LY | | 8.76(4) | 8.77(4) | 8.72(4) | 8.61(5) | 8.46(7) |
| Dzeta | | 0.5999(9) | 0.5990(9) | 0.5982(9) | 0.598(1) | 0.597(1) |
| St400 | | -0.0396(5) | -0.0395(5) | -0.0392(6) | -0.0416(7) | -0.046(1) |
| St220 | | 0.1978(4) | 0.1978(4) | 0.1988(4) | 0.1998(4) | 0.2027(6) |
| $U_{\text{iso}}(\text{Te})$ | | 0.01404(2) | 0.01403(2) | 0.01410(2) | 0.01449(3) | 0.01527(4) |
| $U_{\text{iso}}(\text{Pb})$ | | 0.01398(1) | 0.01539(1) | 0.01967(2) | 0.02712(2) | 0.03803(4) |
| Scale | | 0.21841(2) | 0.21875(2) | 0.21996(2) | 0.22213(3) | 0.22538(4) |

Ba₈Ga₁₆Sn₃₀

| | | Simulation | | Experimental |
|--|------------------------|------------|------------|--------------|
| Temperature (K) | 100 | 300 | 100 | 300 |
| N_{par} | 17 | 17 | 18 | 18 |
| N_{obs} | 1452 | 1464 | 1452 | 1464 |
| $N_{\text{obs}} (I_{\text{obs}} > 3\sigma_{\text{obs}})$ | 1099 | 922 | 1130 | 938 |
| R_F/wR_F (%) | 7.52/9.04 | 7.08/6.20 | 7.31/9.22 | 6.61/6.35 |
| $R_F/wR_F (I_{\text{obs}} > 3\sigma_{\text{obs}})$ (%) | 5.85/8.94 | 4.21/5.96 | 6.02/8.92 | 4.16/5.62 |
| R_{internal} | - | - | 3.9 | 4.41 |
| Extinction | - | - | 0.01(2) | 0.11(2) |
| Ba(1) 2a | $U_{11}(\text{\AA}^2)$ | 0.0110(3) | 0.0219(2) | 0.0110(3) |
| Ba(2) 6d | $U_{11}(\text{\AA}^2)$ | 0.031(2) | 0.047(1) | 0.016(1) |
| | $U_{22}(\text{\AA}^2)$ | 0.205(4) | 0.188(2) | 0.220(4) |
| Sn/Ga(1) 6c | $a[\text{Sn}1]$ | 0.042(2) | 0.044(1) | 0.042(2) |
| | $U_{11}(\text{\AA}^2)$ | 0.0130(7) | 0.0218(6) | 0.0130(7) |
| | $U_{22}(\text{\AA}^2)$ | 0.0124(5) | 0.0201(4) | 0.0122(5) |
| Sn/Ga(2) 16i | $a[\text{Sn}2]$ | 0.217(3) | 0.214(2) | 0.217(3) |
| | x | 0.18408(4) | 0.18419(3) | 0.18411(4) |
| | $U_{11}(\text{\AA}^2)$ | 0.0103(2) | 0.0184(1) | 0.0102(2) |
| | $U_{12}(\text{\AA}^2)$ | -0.0001(1) | -0.0007(1) | -0.0001(1) |
| Sn/Ga(3) 24k | y | 0.31231(5) | 0.31224(4) | 0.31231(5) |
| | z | 0.11837(5) | 0.11839(4) | 0.11836(5) |
| | $U_{11}(\text{\AA}^2)$ | 0.0124(3) | 0.0213(2) | 0.0123(3) |
| | $U_{22}(\text{\AA}^2)$ | 0.0097(2) | 0.0175(2) | 0.0097(2) |
| | $U_{33}(\text{\AA}^2)$ | 0.0093(2) | 0.0167(2) | 0.0094(2) |
| | $U_{23}(\text{\AA}^2)$ | -0.0008(2) | -0.0012(1) | -0.0007(2) |
| | | | | -0.0013(1) |

Integrated charges

PbTe

Table 6 Charge integrated for PbTe NXMEM calculations based on uniform prior

| x | 100 K | | | | 300 K | | | |
|------|------------|--------------|------------|--------------|------------|--------------|------------|--------------|
| | Pb | | Te | | Pb | | Te | |
| | Charge (e) | Multiplicity |
| 0 | 81.88 | 1 | 51.90 | 1 | 81.33529 | 1 | 51.48662 | 1 |
| 0.01 | 81.84 | 1 | 51.89 | 1 | 81.85231 | 1 | 51.91797 | 1 |
| 0.02 | 81.89 | 1 | 52.03 | 1 | 81.41124 | 1 | 51.55936 | 1 |
| 0.03 | 13.62 | 6 | 52.06 | 1 | 81.54675 | 1 | 51.59417 | 1 |
| 0.04 | 12.29 | 6 | 0.84 | | 13.50315 | 6 | 51.92392 | 1 |

We note that the integrated charge of Te at 100 K, $x = 0.04$ are far from correct. This is because the atomic basins are ill defined due to the artefacts seen in Figure 4. This issue can be solved by using a non-uniform prior, Table 7. For $x = 0.03, T = 100 \text{ K}$ the total charge of Pb ($6 \cdot 13.62 = 81.72$) remains in excellent agreement with the nominal value of 82. For $x = 0.04, T = 100 \text{ K}$ the agreement slightly worsens ($6 \cdot 12.29 = 73.74$), however this is also ameliorated by the non-uniform prior, Table 7.

Table 7 Charge integrated for PbTe NXMEM calculations based on non-uniform prior

| x | 100 K | | | | 300 K | | | |
|------|------------|--------------|------------|--------------|------------|--------------|------------|--------------|
| | Pb | | Te | | Pb | | Te | |
| | Charge (e) | Multiplicity |
| 0 | 81.99 | 1 | 52.01 | 1 | 81.97061 | 1 | 52.02461 | 1 |
| 0.01 | 81.97 | 1 | 52.03 | 1 | 81.96862 | 1 | 52.02237 | 1 |
| 0.02 | 81.94 | 1 | 52.06 | 1 | 81.97877 | 1 | 52.01696 | 1 |
| 0.03 | 13.62 | 6 | 52.09 | 1 | 81.94157 | 1 | 52.05444 | 1 |
| 0.04 | 13.49 | 6 | 51.91 | 1 | 13.50492 | 6 | 52.02378 | 1 |

Ba₈Ga₁₆Sn₃₀

Table 8 Positions and charges of each atomic site in the model structures.

| X | Y | Z | Charge (e) | 100 K | | | | 300 K | | | |
|----------|---------|---------|------------|-------|---|---|------------|---------|---------|---------|------------|
| | | | | X | Y | Z | Charge (e) | X | Y | Z | Charge (e) |
| Ba1 | 0 | 0 | 56 | | | | | 0 | 0 | 0 | 56 |
| Ba2 | 0.25427 | 0.54091 | 14 | | | | | 0.25384 | 0.53781 | 0 | 14 |
| Sn/Ga(1) | 0.25 | 0.5 | 37.12545 | | | | | 0.25 | 0 | 0.5 | 37.34889 |
| Sn/Ga(2) | 0.18410 | 0.18410 | 43.43725 | | | | | 0.18419 | 0.18419 | 0.18419 | 43.34098 |
| Sn/Ga(3) | 0 | 0.31241 | 44.92715 | | | | | 0 | 0.31230 | 0.11836 | 44.93547 |

The position of the local density maximum, ($x_{\max}, y_{\max}, z_{\max}$), and corresponding density have been calculated by EDMA. For each maximum is the atomic basin determined. For basin are the centre-of-charge ($x_{\text{coc}}, y_{\text{coc}}, z_{\text{coc}}$) and total charge and volume calculated.

Table 9 Results of topological analysis of NXMEM densities. Full simulated $\text{Ba}_8\text{Ga}_{16}\text{Sn}_{30}$ dataset

| 100K | | | | | | | Charge (e) | Density ($e/\text{\AA}^3$) | Volume (\AA^3) | |
|----------|------------|------------|------------|------------------|------------------|------------------|---------------|---------------------------------|------------------------------|------|
| | x_{\max} | y_{\max} | z_{\max} | x_{coc} | y_{coc} | z_{coc} | multiplicity | | | |
| Ba1 | 0.00000 | 0.00000 | 0.00000 | 0.00000 | 0.00000 | 0.00000 | 2 | 55.10 | 2646.30 | 1.49 |
| Ba2 | 0.25340 | 0.53942 | 0.00000 | 0.25431 | 0.54101 | 0.00017 | 24 | 13.59 | 154.12 | 2.41 |
| Sn/Ga(1) | 0.25000 | 0.00000 | 0.50000 | 0.25000 | 0.00000 | 0.50000 | 6 | 36.80 | 1560.03 | 2.25 |
| Sn/Ga(2) | 0.18416 | 0.18416 | 0.18416 | 0.18408 | 0.18408 | 0.18408 | 16 | 42.83 | 2324.95 | 1.26 |
| Sn/Ga(3) | 0.00000 | 0.31300 | 0.11829 | 0.00000 | 0.31232 | 0.11837 | 24 | 44.43 | 2253.09 | 1.27 |

| 300 K | | | | | | | | | | |
|----------|------------|------------|------------|------------------|------------------|------------------|--------------|---------------|---------------------------------|------|
| | x_{\max} | y_{\max} | z_{\max} | x_{coc} | y_{coc} | z_{coc} | multiplicity | Charge (e) | Density ($e/\text{\AA}^3$) | |
| Ba1 | 0.00394 | 0.00000 | 0.00000 | 0.98306 | 0.00034 | 0.00025 | 12 | 3.64 | 718.90 | 0.19 |
| Ba2 | 0.25887 | 0.54597 | 0.00000 | 0.25375 | 0.53849 | 0.00054 | 24 | 13.14 | 69.95 | 2.16 |
| Sn/Ga(1) | 0.25000 | 0.00000 | 0.50000 | 0.25000 | 0.00000 | 0.50000 | 6 | 36.19 | 578.95 | 1.88 |
| Sn/Ga(2) | 0.18369 | 0.18369 | 0.18369 | 0.18419 | 0.18419 | 0.18419 | 16 | 41.93 | 811.93 | 1.69 |
| Sn/Ga(3) | 0.00000 | 0.30996 | 0.11944 | 0.00000 | 0.31229 | 0.11837 | 24 | 43.66 | 781.96 | 1.80 |

Table 10 Results of topological analysis of NXMEM densities. Low resolution simulated $\text{Ba}_8\text{Ga}_{16}\text{Sn}_{30}$ dataset

| 100K | | | | | | | Charge (e) | Density ($e/\text{\AA}^3$) | Volume (\AA^3) | |
|----------|------------|------------|------------|------------------|------------------|------------------|---------------|---------------------------------|------------------------------|------|
| | x_{\max} | y_{\max} | z_{\max} | x_{coc} | y_{coc} | z_{coc} | multiplicity | | | |
| Ba1 | 0.00000 | 0.00000 | 0.00000 | 0.00000 | 0.00000 | 0.00000 | 2 | 55.62 | 3573.32 | 5.22 |
| Ba2 | 0.25331 | 0.54227 | 0.00000 | 0.25383 | 0.54074 | 0.00058 | 24 | 13.92 | 106.84 | 6.24 |
| Sn/Ga(1) | 0.25000 | 0.00000 | 0.50000 | 0.25000 | 0.00000 | 0.50000 | 6 | 36.97 | 2110.52 | 3.98 |
| Sn/Ga(2) | 0.18411 | 0.18411 | 0.18411 | 0.18407 | 0.18407 | 0.18407 | 16 | 43.30 | 2526.22 | 4.90 |
| Sn/Ga(3) | 0.00000 | 0.31247 | 0.11837 | 0.00000 | 0.31241 | 0.11838 | 24 | 44.89 | 2669.73 | 5.21 |

| 300 K | | | | | | | | | | |
|----------|------------|------------|------------|------------------|------------------|------------------|--------------|---------------|---------------------------------|-------|
| | x_{\max} | y_{\max} | z_{\max} | x_{coc} | y_{coc} | z_{coc} | multiplicity | Charge (e) | Density ($e/\text{\AA}^3$) | |
| Ba1 | 0.00000 | 0.00000 | 0.00000 | 0.00000 | 0.00000 | 0.00000 | 2 | 55.77 | 1274.66 | 7.79 |
| Ba2 | 0.25284 | 0.53826 | 0.00000 | 0.25330 | 0.53901 | 0.00055 | 24 | 13.94 | 71.95 | 5.36 |
| Sn/Ga(1) | 0.25000 | 0.00000 | 0.50000 | 0.25000 | 0.00000 | 0.50000 | 6 | 37.20 | 1027.81 | 11.48 |
| Sn/Ga(2) | 0.18438 | 0.18438 | 0.18438 | 0.18421 | 0.18421 | 0.18421 | 16 | 43.11 | 1301.73 | 7.26 |
| Sn/Ga(3) | 0.00000 | 0.31238 | 0.11894 | 0.00000 | 0.31229 | 0.11842 | 24 | 44.85 | 1358.36 | 8.51 |

Table 11 Results of topological analysis of NXMEM densities. Full experimental $\text{Ba}_8\text{Ga}_{16}\text{Sn}_{30}$ dataset

| 100 K | x_{\max} | y_{\max} | z_{\max} | x_{coc} | y_{coc} | z_{coc} | multiplicity | Charge (e) | Density ($e/\text{\AA}^3$) | Volume (\AA^3) |
|--------------|------------|------------|------------|------------------|------------------|------------------|--------------|------------|------------------------------|---------------------------|
| Ba1 | 0.00000 | 0.00000 | 0.00000 | 0.00000 | 0.00000 | 0.00000 | 2 | 54.21 | 3135.53 | 1.40 |
| Ba2 | 0.25687 | 0.55071 | 0.00000 | 0.25422 | 0.54026 | 0.00089 | 24 | 12.74 | 187.66 | 1.50 |
| Sn/Ga(1) | 0.25000 | 0.00000 | 0.50000 | 0.25000 | 0.00000 | 0.50000 | 6 | 35.51 | 1984.86 | 1.50 |
| Sn/Ga(2) | 0.18428 | 0.18428 | 0.18428 | 0.18410 | 0.18410 | 0.18410 | 16 | 41.67 | 3082.12 | 1.30 |
| Sn/Ga(3) | 0.00000 | 0.31313 | 0.11836 | 0.00000 | 0.31227 | 0.11843 | 24 | 43.28 | 3066.88 | 1.37 |

| 300 K | - | - | - | - | - | - | - | - | - | - |
|--------------|---------|---------|---------|---------|---------|---------|----|-------|--------|------|
| Ba1 | 0.00400 | 0.00400 | 0.00400 | 0.99893 | 0.99920 | 0.99925 | 16 | 37.81 | 701.02 | 1.47 |
| Ba2 | 0.25673 | 0.54922 | 0.00000 | 0.25378 | 0.53859 | 0.00124 | 24 | 11.93 | 79.78 | 1.62 |
| Sn/Ga(1) | 0.25000 | 0.00000 | 0.50000 | 0.25000 | 0.00000 | 0.50000 | 6 | 34.39 | 736.38 | 1.68 |
| Sn/Ga(2) | 0.18472 | 0.18472 | 0.18472 | 0.18412 | 0.18412 | 0.18412 | 16 | 40.42 | 891.74 | 1.43 |
| Sn/Ga(3) | 0.00000 | 0.31403 | 0.11782 | 0.00000 | 0.31221 | 0.11844 | 24 | 41.93 | 933.71 | 1.58 |

Table 12 Results of topological analysis of NXMEM densities. Low resolution experimental $\text{Ba}_8\text{Ga}_{16}\text{Sn}_{30}$ dataset

| 100 K | x_{\max} | y_{\max} | z_{\max} | x_{coc} | y_{coc} | z_{coc} | multiplicity | Charge (e) | Density ($e/\text{\AA}^3$) | Volume (\AA^3) |
|--------------|------------|------------|------------|------------------|------------------|------------------|--------------|------------|------------------------------|---------------------------|
| Ba1 | 0.00000 | 0.00000 | 0.00000 | 0.00000 | 0.00000 | 0.00000 | 2 | 54.75 | 5967.21 | 5.72 |
| Ba2 | 0.25490 | 0.54534 | 0.00000 | 0.25420 | 0.54127 | 0.00099 | 24 | 13.79 | 145.47 | 4.91 |
| Sn/Ga(1) | 0.25000 | 0.00000 | 0.50000 | 0.25000 | 0.00000 | 0.50000 | 6 | 37.07 | 2047.60 | 3.46 |
| Sn/Ga(2) | 0.18435 | 0.18435 | 0.18435 | 0.18403 | 0.18403 | 0.18403 | 16 | 42.98 | 3439.04 | 4.32 |
| Sn/Ga(3) | 0.00000 | 0.31275 | 0.11872 | 0.00000 | 0.31231 | 0.11840 | 24 | 44.62 | 3350.18 | 5.00 |

| 300 K | Ba1 | 0.00000 | 0.00000 | 0.00000 | 0.00000 | 0.00000 | 0.00000 | 2 | 54.80 | 1553.72 | 8.06 |
|--------------|---------|---------|---------|---------|---------|---------|---------|----|-------|---------|-------|
| Ba2 | 0.24986 | 0.52430 | 0.02547 | 0.25009 | 0.52818 | 0.96846 | - | 24 | 8.75 | 79.83 | 2.11 |
| Sn/Ga(1) | 0.25000 | 0.00000 | 0.50000 | 0.25000 | 0.00000 | 0.50000 | - | 6 | 37.02 | 979.58 | 5.49 |
| Sn/Ga(2) | 0.18470 | 0.18470 | 0.18470 | 0.18391 | 0.18391 | 0.18391 | - | 16 | 43.16 | 1473.41 | 16.73 |
| Sn/Ga(3) | 0.00000 | 0.31296 | 0.11880 | 0.00000 | 0.31223 | 0.11834 | - | 24 | 44.38 | 1464.64 | 5.79 |

Initial BayMEM R-values for non-uniform prior

Below are the initial agreement factors reported for MEM and NXMEM calculations on PbTe which were started from non-uniform priors based.

Table 13. PbTe, NXMEM

$T = 100 \text{ K}, U_{\text{iso}} = 0.0053 \text{ \AA}^2$

| x | χ^2 | R | Rw | RF | RFw | RG | RGw |
|------|----------|--------|--------|--------|--------|--------|--------|
| 0 | 0.018162 | 0.0028 | 0.0023 | 0.003 | 0.0021 | 0.0026 | 0.0025 |
| 0.01 | 0.017754 | 0.0026 | 0.0024 | 0.0026 | 0.0018 | 0.0026 | 0.0026 |
| 0.02 | 0.07474 | 0.0085 | 0.0053 | 0.0088 | 0.0036 | 0.008 | 0.0063 |
| 0.03 | 0.6306 | 0.0281 | 0.0171 | 0.0235 | 0.0111 | 0.035 | 0.0216 |
| 0.04 | 8.608 | 0.1007 | 0.0725 | 0.0467 | 0.0366 | 0.1774 | 0.105 |

$T = 300 \text{ K}, U_{\text{iso}} = 0.014 \text{ \AA}^2$

| x | χ^2 | R | Rw | RF | RFw | RG | RGw |
|------|----------|--------|--------|--------|--------|--------|--------|
| 0 | 0.012433 | 0.0031 | 0.002 | 0.003 | 0.0018 | 0.0032 | 0.0022 |
| 0.01 | 0.018928 | 0.003 | 0.0025 | 0.0021 | 0.0018 | 0.0046 | 0.003 |
| 0.02 | 0.05106 | 0.0066 | 0.0044 | 0.006 | 0.0034 | 0.0076 | 0.0054 |
| 0.03 | 0.2355 | 0.0165 | 0.0102 | 0.0133 | 0.0075 | 0.0233 | 0.0132 |
| 0.04 | 0.8391 | 0.0412 | 0.0215 | 0.0296 | 0.0171 | 0.0664 | 0.028 |

Table 14. PbTe, MEM

$T = 100 \text{ K}, U_{\text{iso}} = 0.0053 \text{ \AA}^2$

| x | χ^2 | R | Rw | RF | RFw | RG | RGw |
|------|----------|--------|--------|--------|--------|--------|--------|
| 0 | 0.015979 | 0.002 | 0.0021 | 0.0018 | 0.0019 | 0.0022 | 0.0023 |
| 0.01 | 0.012413 | 0.0019 | 0.0019 | 0.0017 | 0.0015 | 0.0022 | 0.0022 |
| 0.02 | 0.07272 | 0.0059 | 0.0052 | 0.0054 | 0.0035 | 0.0068 | 0.0061 |
| 0.03 | 0.6167 | 0.019 | 0.0168 | 0.0147 | 0.0111 | 0.028 | 0.0213 |
| 0.04 | 2189 | 0.0697 | 1.1468 | 0.0331 | 0.033 | 0.1483 | 1.7824 |

$T = 300 \text{ K}, U_{\text{iso}} = 0.014 \text{ \AA}^2$

| x | χ^2 | R | Rw | RF | RFw | RG | RGw |
|------|----------|--------|--------|--------|--------|--------|--------|
| 0 | 0.012763 | 0.0022 | 0.002 | 0.0019 | 0.0017 | 0.0028 | 0.0022 |
| 0.01 | 0.017028 | 0.002 | 0.0024 | 0.0012 | 0.0015 | 0.0038 | 0.003 |
| 0.02 | 0.04966 | 0.0045 | 0.0043 | 0.0037 | 0.0032 | 0.0068 | 0.0053 |
| 0.03 | 0.2304 | 0.0111 | 0.0101 | 0.0084 | 0.0075 | 0.019 | 0.013 |
| 0.04 | 0.8536 | 0.0279 | 0.0216 | 0.0195 | 0.0171 | 0.0549 | 0.0281 |

BayMEM final R-values

The following tables list the agreement factors reported in the *BayMEM* output for all converged MEM and NXMEM calculations.

Table 15, PbTe, NXMEM

| Uniform prior density | | | | | | | | |
|--|----------|--------|----------|----------|----------|----------|----------|----------|
| $T = 100 \text{ K}, U_{\text{iso}} = 0.0053 \text{ \AA}^2$ | | | | | | | | |
| x | χ^2 | Test | R | Rw | RF | RFw | RG | RGw |
| 0 | 0.018 | 0.8446 | 3.19E-03 | 2.31E-03 | 3.84E-03 | 2.38E-03 | 2.34E-03 | 2.27E-03 |
| 0.01 | 0.014 | 0.8516 | 2.97E-03 | 2.10E-03 | 3.44E-03 | 2.11E-03 | 2.33E-03 | 2.09E-03 |
| 0.02 | 0.029 | 0.6765 | 5.46E-03 | 3.30E-03 | 6.20E-03 | 2.45E-03 | 4.36E-03 | 3.85E-03 |
| 0.03 | 0.055 | 0.5714 | 8.26E-03 | 5.04E-03 | 6.72E-03 | 3.34E-03 | 1.06E-02 | 6.35E-03 |
| 0.04 | 0.58 | 0 | 2.88E-02 | 1.88E-02 | 2.08E-02 | 7.21E-03 | 4.00E-02 | 2.83E-02 |

| $T = 300 \text{ K}, U_{\text{iso}} = 0.014 \text{ \AA}^2$ | | | | | | | | |
|---|----------|--------|----------|----------|----------|----------|----------|----------|
| x | χ^2 | Test | R | Rw | RF | RFw | RG | RGw |
| 0 | 0.04 | 0.8274 | 4.66E-03 | 3.61E-03 | 5.22E-03 | 4.56E-03 | 3.67E-03 | 2.45E-03 |
| 0.01 | 0.013 | 0.5488 | 2.62E-03 | 2.10E-03 | 2.16E-03 | 1.55E-03 | 3.45E-03 | 2.50E-03 |
| 0.02 | 0.04 | 0.7816 | 6.09E-03 | 3.93E-03 | 6.42E-03 | 4.13E-03 | 5.46E-03 | 3.69E-03 |
| 0.03 | 0.06 | 0.6876 | 9.36E-03 | 5.17E-03 | 7.34E-03 | 4.62E-03 | 1.36E-02 | 5.87E-03 |
| 0.04 | 0.088 | 0.3929 | 1.46E-02 | 6.99E-03 | 9.16E-03 | 4.55E-03 | 2.63E-02 | 1.01E-02 |

Table 16, PbTe, NXMEM

| Nonuniform prior density | | | | | | | | |
|--|----------|--------|----------|----------|----------|----------|----------|----------|
| $T = 100 \text{ K}, U_{\text{iso}} = 0.0053 \text{ \AA}^2$ | | | | | | | | |
| x | χ^2 | Test | R | Rw | RF | RFw | RG | RGw |
| 0 | 0.013 | 0.3122 | 2.42E-03 | 1.94E-03 | 2.81E-03 | 1.86E-03 | 1.93E-03 | 1.99E-03 |
| 0.01 | 0.01 | 0.2716 | 2.33E-03 | 1.77E-03 | 2.55E-03 | 1.56E-03 | 2.04E-03 | 1.90E-03 |
| 0.02 | 0.029 | 0.6596 | 5.55E-03 | 3.28E-03 | 6.31E-03 | 2.46E-03 | 4.43E-03 | 3.81E-03 |
| 0.03 | 0.065 | 0.6104 | 8.67E-03 | 5.46E-03 | 7.51E-03 | 3.83E-03 | 1.04E-02 | 6.76E-03 |
| 0.04 | 0.543 | 0.1713 | 2.49E-02 | 1.82E-02 | 1.91E-02 | 7.73E-03 | 3.32E-02 | 2.71E-02 |

| $T = 300 \text{ K}, U_{\text{iso}} = 0.014 \text{ \AA}^2$ | | | | | | | | |
|---|----------|--------|----------|----------|----------|----------|----------|----------|
| x | χ^2 | Test | R | Rw | RF | RFw | RG | RGw |
| 0 | 0.01 | 0.3544 | 2.79E-03 | 1.81E-03 | 2.61E-03 | 1.60E-03 | 3.09E-03 | 1.98E-03 |
| 0.01 | 0.012 | 0.2324 | 2.34E-03 | 2.05E-03 | 1.72E-03 | 1.35E-03 | 3.46E-03 | 2.53E-03 |
| 0.02 | 0.04 | 0.747 | 6.11E-03 | 3.93E-03 | 5.69E-03 | 3.12E-03 | 6.94E-03 | 4.69E-03 |
| 0.03 | 0.1 | 0.5633 | 1.08E-02 | 6.67E-03 | 9.29E-03 | 5.74E-03 | 1.39E-02 | 7.82E-03 |
| 0.04 | 0.09 | 0.2769 | 1.46E-02 | 7.04E-03 | 9.16E-03 | 4.60E-03 | 2.64E-02 | 1.02E-02 |

Table 17, PbTe, MEM

Uniform prior density

| $T = 100 \text{ K}, U_{\text{iso}} = 0.0053 \text{ \AA}^2$ | | | | | | | | | |
|--|----------|--------|----------|----------|----------|----------|----------|----------|--|
| oc | χ^2 | Test | R | Rw | RF | RFw | RG | RGw | |
| 0 | 0.002 | 0.0053 | 0.001037 | 0.000794 | 0.001369 | 0.001147 | 0.000482 | 0.000473 | |
| 0.01 | 0.002 | 0.0039 | 0.001116 | 0.000782 | 0.001407 | 0.001088 | 0.000609 | 0.000513 | |
| 0.02 | 0.004 | 0.0119 | 0.001984 | 0.00121 | 0.002637 | 0.001678 | 0.000715 | 0.00065 | |
| 0.03 | 0.003 | 0.0076 | 0.001749 | 0.001175 | 0.001646 | 0.001084 | 0.001969 | 0.001263 | |
| 0.04 | 11 | 1.0818 | 0.1049 | 0.08256 | 0.08513 | 0.08137 | 0.1476 | 0.0842 | |

| $T = 300 \text{ K}, U_{\text{iso}} = 0.014 \text{ \AA}^2$ | | | | | | | | | |
|---|----------|--------|----------|----------|----------|----------|----------|----------|--|
| oc | χ^2 | Test | R | Rw | RF | RFw | RG | RGw | |
| 0 | 0.002 | 0.017 | 0.001027 | 0.0008 | 0.001118 | 0.000955 | 0.000818 | 0.000633 | |
| 0.01 | 0.002 | 0.0122 | 0.001141 | 0.000813 | 0.001208 | 0.000987 | 0.000985 | 0.000618 | |
| 0.02 | 0.003 | 0.0422 | 0.001362 | 0.00106 | 0.001332 | 0.001058 | 0.001443 | 0.001063 | |
| 0.03 | 0.002 | 0.0447 | 0.001589 | 0.000961 | 0.001691 | 0.001093 | 0.001291 | 0.000731 | |
| 0.04 | 0.019 | 0.0182 | 0.005006 | 0.003192 | 0.003271 | 0.001968 | 0.01058 | 0.004664 | |

Table 18, PbTe, MEM

Nonuniform prior density

| $T = 100 \text{ K}, U_{\text{iso}} = 0.0053 \text{ \AA}^2$ | | | | | | | | | |
|--|----------|--------|----------|----------|----------|----------|----------|----------|--|
| oc | χ^2 | Test | R | Rw | RF | RFw | RG | RGw | |
| 0 | 0.003 | 0.0952 | 0.001062 | 0.000935 | 0.001297 | 0.001237 | 0.000669 | 0.000696 | |
| 0.01 | 0.002 | 0.1533 | 0.001035 | 0.000782 | 0.00113 | 0.000796 | 0.000869 | 0.000773 | |
| 0.02 | 0.003 | 0.1494 | 0.001829 | 0.001078 | 0.002191 | 0.001201 | 0.001124 | 0.000974 | |
| 0.03 | 0.005 | 0.0655 | 0.002042 | 0.001566 | 0.001659 | 0.001185 | 0.002858 | 0.001885 | |
| 0.04 | 0.4 | 0.0206 | 0.02204 | 0.01554 | 0.01588 | 0.01069 | 0.03529 | 0.02054 | |

| $T = 300 \text{ K}, U_{\text{iso}} = 0.014 \text{ \AA}^2$ | | | | | | | | | |
|---|----------|--------|----------|----------|----------|----------|----------|----------|---|
| oc | χ^2 | Test | R | Rw | RF | RFw | RG | RGw | |
| 0 | - | - | - | - | - | - | - | - | - |
| 0.01 | 0.001 | 0.2216 | 0.000792 | 0.000575 | 0.000818 | 0.000654 | 0.00073 | 0.000494 | |
| 0.02 | 0.002 | 0.2487 | 0.000981 | 0.000872 | 0.000886 | 0.00079 | 0.001228 | 0.000956 | |
| 0.03 | 0.001 | 0.2342 | 0.001186 | 0.000741 | 0.001237 | 0.000828 | 0.001038 | 0.000593 | |
| 0.04 | 0.015 | 0.0371 | 0.004288 | 0.002825 | 0.002524 | 0.0014 | 0.009953 | 0.00436 | |

Table 19, Ba₈Ga₁₆Sn₃₀, NXMEM

| Simulated data | | | | | | | | |
|----------------|----------|--------|--------|--------|--------|--------|--------|--------|
| Full dataset | | | | | | | | |
| T (K) | χ^2 | Test | R | Rw | RF | RFw | RG | RGw |
| 100 | 1.8000 | 0.4457 | 0.0204 | 0.0255 | 0.0204 | 0.0255 | 0.0000 | 0.0000 |
| 300 | 1.2000 | 0.5553 | 0.0270 | 0.0221 | 0.0270 | 0.0221 | 0.0000 | 0.0000 |

| Low resolution | | | | | | | | |
|----------------|----------|--------|--------|--------|--------|--------|--------|--------|
| T (K) | χ^2 | Test | R | Rw | RF | RFw | RG | RGw |
| 100 | 0.5990 | 0.5648 | 0.0086 | 0.0096 | 0.0086 | 0.0096 | 0.0000 | 0.0000 |
| 300 | 0.1240 | 0.2853 | 0.0043 | 0.0044 | 0.0043 | 0.0044 | 0.0000 | 0.0000 |

Table 20, Ba₈Ga₁₆Sn₃₀, MEM

| Experimental data | | | | | | | | |
|-------------------|----------|--------|--------|--------|--------|--------|--------|--------|
| Full dataset | | | | | | | | |
| T (K) | χ^2 | Test | R | Rw | RF | RFw | RG | RGw |
| 100 | 3.9910 | 0.6706 | 0.0322 | 0.0383 | 0.0322 | 0.0383 | 0.0000 | 0.0000 |
| 300 | 3.9560 | 0.6937 | 0.0394 | 0.0405 | 0.0394 | 0.0405 | 0.0000 | 0.0000 |

| Low resolution | | | | | | | | |
|----------------|----------|--------|--------|--------|--------|--------|--------|--------|
| T (K) | χ^2 | Test | R | Rw | RF | RFw | RG | RGw |
| 100 | 0.4450 | 0.2632 | 0.0074 | 0.0083 | 0.0074 | 0.0083 | 0.0000 | 0.0000 |
| 300 | 0.4490 | 0.2739 | 0.0072 | 0.0084 | 0.0072 | 0.0084 | 0.0000 | 0.0000 |

References

- Bindzus, N. & Iversen, B. B. (2012). *Acta Cryst. A* **68**, 750-762.
- Christensen, S., Avila, M. A., Suekuni, K., Piltz, R., Takabatake, T. & Christensen, M. (2013). *Dalton Trans.* **42**, 14766.
- Hofmann, A., Netzel, J. & van Smaalen, S. (2007). *Acta Cryst. B* **63**, 285-295.
- Kuhs, W. F. (2003). *International Tables for Crystallography* edited by A. Authier, pp. 228-242.
Dordrecht/Boston/London: Kluwer Academic Publisher.
- Palatinus, L., Prathapa, S. J. & van Smaalen, S. (2012). *J. Appl. Crystallogr.* **45**, 575-580.
- van Smaalen, S., Palatinus, L. & Schneider, M. (2003). *Acta Cryst. A* **59**, 459-469.